Journal of Harbin Engineering University Vol 44 No. 7
ISSN: 1006-7043 July 2023

An Application of Advanced Neutrosophic Numbers for Lung Disease Detection

Gokilamani.R[1] Sahaya Sudha.A[2]
[1]Department of Mathematics, Sri Ramakrishna College of Arts & Science for Women, Coimbatore, Tamilnadu. India .
gokila70@gmail.com
[2]Department of Mathematics, Nirmala College for Women, Coimbatore, Tamilnadu. India
sudha.dass@yahoo.com

ABSTRACT
Lung disease is one of the diseases that can be cured when the disease is detected in its early stages before it get progressed. Early diagnosis can be promising to curable. But, the most people fail to detect their disease before it comes to chronic. It leads to an increases in the death rate all around the world. Hence, an efficient model is required for the early detection and classification of lung diseases and its types. Generally, the Chest X-ray (CXR) are used to predict the different types of lung diseases like lung cancer, pneumonia, COVID-19 etc. But, the CXR images consist of fuzzy and imprecision information that makes segmentation and classification a difficult task. Thus, the generalizations of fuzzy sets are used utilized to reduce the fuzziness and uncertainty in images. Fuzzy methods fails to consider the spatial pixel data due to noise and artifacts which play a vital role in many real-time applications. To resolve this, Consecutive Neutrosophic Set (CNSS) approach with Deep Learning (DL) model (CNSDL) is developed for lung diseases. In this model, Bipolar Trapezoidal Double Refined Indeterminate Neutrosophic Set (BTDRINSS) and Gaussian based Bipolar Trapezoidal Double Refined Indeterminate Neutrosophic Set (GBTDRINSS) is developed and employed along with the original NSS for the prediction tasks. The suggested model is categorized into three stages. Initially, the input CXRimages are converted to three NS domain with True (T), False (F) and Indeterminacy (I) set images individually which reduces the fuzziness and retain more significant information for feature extraction of the opacity to distinguish the types of lung diseases.The entropy in three NS domain is applied to evaluate the indeterminacy. Then, the two operations like α −mean and β −enhancement operations are used to reduce the set indeterminacy to enhance the image edges to improve accuracy. In addition, K − means clustering method is utilized for the image segmentation tasks. Finally, the enhanced image features are given as input to the DL model (ResNet 50) to train and test for the type of lung diseases.The test experimental outcomes show that the proposed GBTDRINSS model provides the accuracy of 97.25% on lung diseases prediction compared to the other existing models.

Keywords: Lung disease, Neutrosophic Set, Deep Learning, Chest X-ray, K-Means Clustering.

1. INTRODUCTION

Lungs play a vital role in the human system, which performs expansion and relaxation to bring in oxygen and take out carbon dioxide. Lung diseases are respiratory diseases that affect the various organs and tissues associated with breathing, leading to airway diseases, lung tissue diseases, and lung circulation diseases [1, 2]. Some of the lung diseases like common cold and influenza cause mild discomfort and hindrance while others like lower respiratorydiseases (pneumonia), tuberculosis (TB), Chronic Obstructive Pulmonary Disease (COPD), lung cancer, COVID-19 are leading causes of respiratory morbidity and mortality among adults pneumonia, tuberculosis and lung cancer are life-threatening and cause severe acute respiratory problems [3]. Therefore, early detection of lung diseases has a major role in increasing the chances of recovery. There are various options in which lung diseases can be detected including blood testing, sputum sample testing, skin testinghaveall been used in the past to detect pulmonary problems [4]. Even though these state-of-the-art imaging techniques yield precise, reliable, and impermeable results, their accessibility and availability are constrained in

underdeveloped countries due to the lack of a strong healthcare system and patient comfort.

Among different imaging techniques like Magnetic Resonance Imaging (MRI), and Computed Tomography (CT) scans and so on, CXR is majorly used and easily available tool to predict the stage to for various diseases diagnosis. Different detection models [5, 6, 7, 8] have been developed to identify the lung diseases and its types using CXR images. But, CXR images in medical classification consists of fuzzy and inaccurate information, making segmentation and categorization problematic. Thus, the generalizations of fuzzy sets are commonly used to minimize the fuzziness and uncertainty in images, and numerous studies have concluded that the fuzzy theory on image enhancement maintains more relevant information than conventional methods [9]. Due to noise and abnormalities, these fuzzy methods ignores the spatial pixel data, which play a crucial role in numerous real-time implementations. To resolve this issue, NS is considered to be the superior method to quantify the images with the usage of indeterminacy.

NS is a subset of neutrosophy theory that investigates the origin, nature, and scope of neutralities, as well as their interaction with various ideational spectra [10]. By generalizing truth, indeterminacy, and false membership, the NS enhances the independent uncertainty measures further. The proposed work concentrates on using a neutrosophic method to minimize fuzziness and conserve more significant information for feature extraction of opacity to differentiate lung diseases such as normal, viral, and bacterial pneumonia as well as COVID-19 infection.

Numerous studies on lung infection detection employ either conventional image segmentation or machine learning (ML) models. But still, manual approach is performed by ML models and does not classify the CXR images effectively leading to misleading results. In recent days, DL models plays an important role in the medical field especially for medical image analysis [11, 12]. Lung disease detection generally deals with classifying an image into healthy lungs or disease-infected lungs. The lung disease classifier sometimes known as a model which is obtained via training. Training is the process in which a neural network learns to recognize a class of images. Using DL, it is possible to train a model that can classify images into their respective class labels. Hence, this framework adopts for DL to provide an efficient classification of lung diseases and its types. The contribution of this research work is illustrated as follows.

1. Initially, the CXR images are collected and it is transformed to NSS, BTDRINSS and GBTDRINSSapproach
2. The Neutrosophic Image (NI) entropy is used to evaluate the indeterminacy and distributes$T$, I, and F eventually into the three NS domain at separate stages.
3. Then, the gathered image from the three NS domain are pre-processed using $\alpha -$ means and $\beta -$ enhancementsoperations to reduce the indeterminacy of the image which is measured by the entropy of the indeterminate set.
4. Next, the pre-processed images are segmentedusing $K -$ means clustering method on NS domain which removes the noises effectively and retain more significant information to improve the prediction accuracy.
5. Finally, the enhanced images are fed into the ResNet - 50 to train and test for the type of lung diseases such as normal, viral, and bacterial pneumonia and COVID-19 infection.

The remaining sections of this article are prepared as follows: Section II discusses recent works associated with lung diseases and its type's identification. Section III explains the presented methodology and Section IV exemplifies its performance. Section V summarizes this work and suggests possible improvements.

2. LITERATURE SURVEY

A method based on weighted classifier was presented [13] for recognizing pneumonia from CXR scans. In this method, the weighted predictions from the classical DL structures were combined. This approach was a supervised learning approach in which the network predicts the result based on the quality of the dataset used. Also, TL model was utilized to

modify the DL and increase detection accuracy. Partial data augmentation techniques were employed to increase the training dataset in a balanced way to improve the model's efficiency. Conversely, the amount of inaccurately labeled images was not limited.

A hybrid deep neural network (DNN) with adaptive sine cosine crow search algorithm (ASCCS)was presented [14] to detect the types of lung cancer. Initially, the preprocessing stage was performed using the fast non local means (FNLM) filter. For the segmentation process, the Masi entropy based multilevel thresholding using salp swarm algorithm (MasiEMT-SSA) was utilized to segment the cancer nodule from the lung images. The binary grasshopper optimization algorithm (BGOA) was applied to select the optimum features for the feature selection (FS) process. Then the selected features were classified using the hybrid classifier named as DNN and ASCCSalgorithm to accurately detect the lung cancer types. However, the However, the accuracy was slightly reduced while processing with full version of dataset.

A parallel Channel Attention feature Fusion (PCAF) scheme called MCFF-Net was suggested [15] according to the characteristics of CXR images. Based on this module, a new CNN structure is proposed to classify CXR images in order to diagnose and detect COVID-19 cases. Also, the recognition efficiency was enhanced fully connected (FC) layers to perform classification experiment on a dataset containing four types of image of COVID-19, normal, bacterial pneumonia, and viral pneumonia. However, this model provides lower performances on larger dataset.

A VGG framework was developed [16] for detecting pneumonia from CXR scans. First, the CXR scans were collected and pre-processed by the Dynamic Histogram Equalization (DHE) technique. Then, VGG-based CNN model was developed to extract the features from original images or previous feature maps which contained only six layers combining ReLU activation function, drop operation, and max-pooling layers. This model effectively capture the characteristics of CXR scans and learn them to recognize whether a person suffers from pneumonia or not. However, this model results in overfitting issues.

A DL model called EfficientNet v2-M was developed [17] for multi-class lung diseases' classification on CXR images. The constructed EfficientNet v2-M model utilizes the pre-trained weights of ImageNet to classify lung diseases on CXR images to improve the efficiency and accuracy of CADs' diagnostic performance. Initially, the data were augmented to increase the number of samples and variance diversities. Then, they were directly inputted into an EfficientNet v2-M model to extract their meaningful features in identifying lung disease categories. But, this model loses a substantial amount of useful data, resulting in overfitting difficulties.

A novel medical image enhancement approach was presented [18] depending on a type-2 neutrosophic set (T2NS) and α-mean and β-enhancement operations for Covid-19 detection. This new approach obtains a good enhancement result by defining the uncertainties within the image in a six-degree membership. Through enhancement operations, T2NS entropy was determined to evaluate the change in the gray level of CXR images. An image de-neutrosophication operation was obtained on the enhanced images to convert them from the NS domain to the grayscale image. However, this model has less generalizability compared to other models

A fuzzy-enhanced DL approach was suggested [19] for early prediction of Covid-19 or other related lung diseases. In this model, customized deep CNN model called calledCovNNet have been developed to perform binary classification. A hybrid architecture was constructed in which block features was extracted from *CovNNet* trained on raw CXR images, and a second block of features is extracted from images pre-processed by fuzzy edge detection method. The two blocks are then combined in a unique vector to train a multilayer feedforward neural network for the automatic detection of Covid-19 and other lung diseases. However, this model necessitates more parameters to optimize the CNN structure.

An Application Method was constructed [20] by utilizing the Neutrosophic Soft Mappings (NSM) approach for the detection of lung diseases

types and select the best therapy modality. This method consists of three modes. Initially, the categories of lung diseases were listed in a table based on the fuzzy interval [0, 1]. Then, a calculation based NSM was constructed to accurately diagnose each patient's infection and select the optimum treatment. In addition, generalized NSM was used to observe the treatment process of the patient throughout the therapy estimate the duration of the treatment. However, this methods provides many confusion results which degrades the performance efficiency.

A Hybrid DL Algorithm (HDLA) framework was presented [21] for automatic lung disease classification from CXR images. The model consists of different stages which includes pre-processing of CXR images, automatic feature extraction, and detection. In a pre-processing step, the CXR images was enhanced using optimal filtering tasks. The robust CNN was developed using the pre-trained model for automatic lung feature extraction. Then, the 2D CNN modelwas used for the optimum feature extraction in minimum time and space requirements. The classifiers like Adaboost and DNN model was used to classify the CXR images. However, this model was more sensitive to noise and outliers data.

3. PROPOSED METHODOLOGY

In this section, the CNSS-DL model is briefly illustrated. Initially, the collected CXR images are transformed into the NSS, BTDRINSS and GBTDRINSS using three membership sets like T, I and F separately.Then, two $\alpha -$ mean and $\beta -$ enhancement operations are proposed to reduce the indeterminacy of the image, which is measured by the entropy of the indeterminate set. The image becomes more uniform and homogenous, and more suitable for segmentation. Next, the image in the NS domain is segmented using $K -$ means clustering method. Finally, the ResNet 50 is employed to classify and predict the different types of lung diseases. The schematic representation of this proposed model is depicted in figure 1.

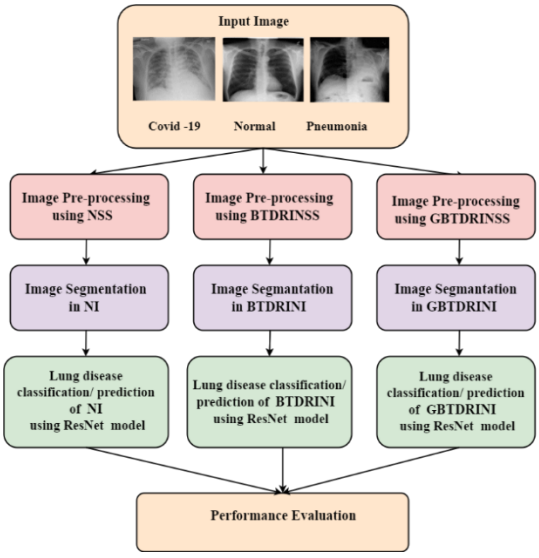

Figure 1 Schematic Representation of the proposed model

3.1 Dataset Description

CXR data [22]: A team of researchers from Qatar University, Doha, Qatar, and the University of Dhaka, Bangladesh along with their collaborators from Pakistan and Malaysia in collaboration with medical doctors have created a database of CXR images for covid-19 positive cases along with normal and viral pneumonia images. This COVID-19, normal, and other lung infection dataset is released in stages. In the first release, we have released 219 COVID-19, 1341 normal, and 1345 viral pneumonia chest X-ray (CXR) images. In the first update, we have increased the COVID-19 class to 1200 CXR images. In the 2nd update, we have increased the database to 3616 COVID-19 positive cases along with 10,192 Normal, 6012 Lung Opacity (Non-COVID lung infection), and 1345 Viral Pneumonia images and corresponding lung masks.

3.2 Neutrosophic Domain

3.2.1 Neutrosophic Set (NSS)

Assume X to be a universe of discourse which contains x. An element x in setNSS(A) is denoted in mathematical terms as $x\ (t, i, f\ )$ and represented in NSS logic using Eq.(1):

$$NSS(A) = \{[x, (T_A(x), I_A(x), F_A(x)]\ x\ \in X\} \quad (1)$$

Where, $T_A(x)$, $I_A(x)$ and $F_A(x)$ are the neutroscopic components and are real standard or non-standard sets of

$]\ 0^-, 1^+[$ and is defined using Eq. (2) – (3)

$$N_{sup} = t_{sup} + i_{sup} + f_{sup}, \quad (2)$$

Where, $\sup\_T = t_{sup}, \sup\_I = i_{sup}, \sup\_F = f_{sup}$

$N_{inf} = t_{inf} + i_{inf} + f_{inf}$,(3)

Where, $\inf\_T = t_{inf}$, $\inf\_I = i_{sup}, \inf\_F = f_{inf}$

So, $0^- \leq T_A(x) + I_A(x) + F_A(x) \leq 3^+$

In the above equations, T, I and F are defined as neutrosophic components. The elements $x\,(t, i, f\,)$ belongs to V is represented in following categories; it is t % true, i % indeterminacy, and f % false, where t varies in T, i varies in I, and f varies in F. Statically, T, I and F are membership sets, but dynamically T, I and $F$are functions/operators depending on known and /or unknown parameters. The sets T, I and $F$are not necessarily intervals, and maybe any real sub-unitary subsets like discrete or continuous; single-element, finite, or countable or uncountable infinite; union or intersection of various subsets; etc.,

3.2.2 BTDRINSS

To enhance the decision-making process in image processing, the BTDRINSShave been formulated with polarity-based membership. The positive and negative Degree of Membership's in BTDRINSS are positive degree of truth membership (${T_A}^+$), positive degree of indeterminate toward truth membership (${I_T}^+(x)$), positive degree of indeterminate toward falsity (${I_F}^+(x)$), positive degree of falsity membership ($F^+(x)$), negative degree of truth-membership ($T^-(x)$), negative degree of indeterminate towards truth membership (${I_T}^-(x)$), negative degree of indeterminate toward falsity (${I_F}^-(x)$), negative degree of falsity membership ($F^-(x)$).

Assume X to be a universe of discourse which contains x in set BTDRINSS(A) is denoted in Eq. (4)

$$BTDRINS\,(A) = \left\{< x, {T_A}^+(x), {I_{A_{T_A}}}^+(x), {I_{A_{F_A}}}^+(x), {F_A}^+(x), {T_A}^-(x), {I_{T_A}}^-(x), {I_{A_{F_A}}}^-(x), {F_A}^-(x) > \right\} \quad (4)$$

Where, ${T_A}^+(x), {I_{A_{T_A}}}^+(x), {I_{A_{F_A}}}^+(x), {F_A}^+(x) \rightarrow$ [0 , 1] (Positive membership degrees)

${T_A}^-(x), {I_{A_{T_A}}}^-(x), {I_{A_{F_A}}}^-(x), {F_A}^-(x) \rightarrow$ [0 , 1] (Negative Membership degrees)

Such that,

$$0 \leq {T_A}^+(x), {I_{T_A}}^+(x), {I_{A_{F_A}}}^+(x), {F_A}^+(x) \leq 3, -30 \leq {T_A}^-(x), {I_{T_A}}^-(x), {I_{A_{F_A}}}^-(x), {F_A}^-(x) \leq 0$$

The above listed positive and negative degree of Membership's values in BTDRINSS is totally modulated from the original NS domain which is used to enhance the decision-making process in image processing. Also, BTDRINSS using the positive and negative degree of falsity membership will remove non-member pixels of given image and later the image can be converted to RGB image.

3.2.3GBTDRINSS

In GBTDRINSS, the bipolarity function works as like the BTDRINSS but the images are undergo Gaussian process before applying membership function. The Gaussian function is very helpful to image pixel veracity enhancement. In GBTDRINSS, the Gaussian function is applied and then the BTDRINSS membership function applied for the image processing. Using the mean and standard deviation (SD) of falsity membership, the non-member pixels of given image is removed and then reverse Gaussian applied to image to remove non familiar pixel removing and later image converted to RGB image Assume, the logic behind GBTDRINSSin Eq. (5)

$$\bar{\bar{A}}_{GN} = \left((\overline{\mu_t}, \sigma_t), (\overline{\mu_{it}}, \sigma_{it}), (\overline{\mu_{if}}, \sigma_f), (\overline{\mu_f}, \sigma_f)\right) \quad (5)$$

The above Eq. (5) represents the truth membership function, indeterminacy leaning towards truth membership function, indeterminacy leaning towards falsity membership function and falsity membership function. The mean and SD of GBTDRINSS is listed in table 1.

Table 1. The mean and SD of GBTDRINSS

Truth Membership Function	**Indeterminacy Leaning towards Truth Membership Function**
$\psi\,(x_t) = \exp\left(-\frac{1}{2}\left(\frac{x_t - \overline{\mu_t}}{\sigma_t}\right)^2\right)$(6(a))	$\psi(x_{it}) = \exp\left(-\frac{1}{2}\left(\frac{x_{it} - \overline{\mu_{it}}}{\sigma_{it}}\right)^2\right)$(6(b))
Indeterminacy Learning Towards Falsity Membership Function	**Falsity Membership Function**

$\psi(x_{if}) = 1 - \exp\left(-\frac{1}{2}\left(\frac{x_{if}-\overline{\mu_{if}}}{\sigma_{if}}\right)^2\right)$(6(c))	$\psi\,(x_f) = 1 - \exp\left(-\frac{1}{2}\left(\frac{x_f-\overline{\mu_f}}{\sigma_f}\right)^2\right)$(6(d))

In above Eq. 6(a), 6(b), 6(c) and 6(d)$\overline{\mu_t}, \overline{\mu_{it}}, \overline{\mu_{if}}, \overline{\mu_f}$denotes the mean of truth membership function, indeterminacy leaning towards truth membership function, indeterminacy leaning towards falsity membership function and falsity membership function value. $\sigma_t, \sigma_{it}, \sigma_{if}, \sigma_f$ denotes the standard deviation of distribution of truth membership function, indeterminacy leaning towards truth membership function, indeterminacy leaning towards falsity membership function and falsity membership value. Mostly, the GBTDRINSS works on the $\alpha - cut$operationsis illustrated in Eq. (7) and (8)

Let $\bar{\bar{\mathcal{A}}}_{GN} = \left((\bar{\mu}_{\bar{\mathcal{A}}_t}, \sigma_{\bar{\mathcal{A}}_t}), \left(\bar{\mu}_{\bar{\mathcal{A}}_{it}}, \sigma_{\bar{\mathcal{A}}_{it}}\right), \left(\bar{\mu}_{\bar{\mathcal{A}}_{if}}, \sigma_{\bar{\mathcal{A}}_{if}}\right), \left(\bar{\mu}_{\bar{\mathcal{A}}_f}, \sigma_{\bar{\mathcal{A}}_f}\right)\right)$ (7)

and

$\bar{\bar{\mathcal{B}}}_{GN} = \left((\bar{\mu}_{\bar{\mathcal{B}}_t}, \sigma_{\bar{\mathcal{B}}_t}), \left(\bar{\mu}_{\bar{\mathcal{B}}_{it}}, \sigma_{\bar{\mathcal{B}}_{it}}\right), \left(\bar{\mu}_{\bar{\mathcal{B}}_{if}}, \sigma_{\bar{\mathcal{B}}_{if}}\right), \left(\bar{\mu}_{\bar{\mathcal{B}}_f}, \sigma_{\bar{\mathcal{B}}_f}\right)\right)$(8)

be two GBTDRINSS domains. Then theirα − cuts of GBTDRINSS are as follows:

$\bar{\bar{\mathcal{A}}}_{GN_{t\alpha}} = \left[\bar{\mu}_{\bar{\mathcal{A}}_t} - \sigma_{\bar{\mathcal{A}}_t}\sqrt{-2\log\alpha}\ ,\ \bar{\mu}_{\bar{\mathcal{A}}_t} + \sigma_{\bar{\mathcal{A}}_t}\sqrt{-2\log\alpha}\right]$ 9(a)

$\bar{\bar{\mathcal{A}}}_{GN_{it\alpha}} = \left[\bar{\mu}_{\bar{\mathcal{A}}_{it}} - \sigma_{\bar{\mathcal{A}}_{it}}\sqrt{-2\log\alpha}\ ,\ \bar{\mu}_{\bar{\mathcal{A}}_{it}} + \sigma_{\bar{\mathcal{A}}_{it}}\sqrt{-2\log\alpha}\right]$ 9(b)

$\bar{\bar{\mathcal{A}}}_{GN_{if\alpha}} = \left[\bar{\mu}_{\bar{\mathcal{A}}_{if}} - \sigma_{\bar{\mathcal{A}}_{if}}\sqrt{-2\log(1-\alpha)}\ ,\ \bar{\mu}_{\bar{\mathcal{A}}_{if}} + \sigma_{\bar{\mathcal{A}}_{if}}\sqrt{-2\log(1-\alpha)}\right]$ 9(c)

$\bar{\bar{\mathcal{A}}}_{GN_{f\alpha}} = \left[\bar{\mu}_{\bar{\mathcal{A}}_f} - \sigma_{\bar{\mathcal{A}}_f}\sqrt{-2\log(1-\alpha)}\ ,\ \bar{\mu}_{\bar{\mathcal{A}}_f} + \sigma_{\bar{\mathcal{A}}_f}\sqrt{-2\log(1-\alpha)}\right]$ 9(d)

and

$\bar{\bar{\mathcal{B}}}_{GN_{t\alpha}} = \left[\bar{\mu}_{\bar{\mathcal{B}}_t} - \sigma_{\bar{\mathcal{B}}_t}\sqrt{-2\log\alpha}\ ,\ \bar{\mu}_{\bar{\mathcal{B}}_t} + \sigma_{\bar{\mathcal{B}}_t}\sqrt{-2\log\alpha}\right]$10(a)

$\bar{\bar{\mathcal{B}}}_{GN_{it\alpha}} = \left[\bar{\mu}_{\bar{\mathcal{B}}_{it}} - \sigma_{\bar{\mathcal{B}}_{it}}\sqrt{-2\log\alpha}\ ,\ \bar{\mu}_{\bar{\mathcal{B}}_{it}} + \sigma_{\bar{\mathcal{B}}_{it}}\sqrt{-2\log\alpha}\right]$10(b)

$\bar{\bar{\mathcal{B}}}_{GN_{if\alpha}} = \left[\bar{\mu}_{\bar{\mathcal{B}}_{if}} - \sigma_{\bar{\mathcal{B}}_{if}}\sqrt{-2\log(1-\alpha)}\ ,\ \bar{\mu}_{\bar{\mathcal{B}}_{if}} + \sigma_{\bar{\mathcal{B}}_{if}}\sqrt{-2\log(1-\alpha)}\right]$10(c)

$\bar{\bar{\mathcal{B}}}_{GN_{f\alpha}} = \left[\bar{\mu}_{\bar{\mathcal{B}}_f} - \sigma_{\bar{\mathcal{B}}_f}\sqrt{-2\log(1-\alpha)}\ ,\ \bar{\mu}_{\bar{\mathcal{B}}_f} + \sigma_{\bar{\mathcal{B}}_f}\sqrt{-2\log(1-\alpha)}\right]$10(d)

Based on α − cuts, the arithmetic operations between $\bar{\bar{\mathcal{A}}}_{GN}$ and $\bar{\bar{\mathcal{B}}}_{GN}$ are defined as follows in addition, subtraction, multiplication and division are defined below.

1. Addition:

$\bar{\bar{\mathcal{A}}}_{GN_{t\alpha}} + \bar{\bar{\mathcal{B}}}_{GN_{t\alpha}} = \left[\left(\bar{\mu}_{\bar{\mathcal{A}}_t} + \bar{\mu}_{\bar{\mathcal{B}}_t}\right) - \left(\sigma_{\bar{\mathcal{A}}_t} + \sigma_{\bar{\mathcal{B}}_t}\right)\sqrt{-2\log\alpha}\ ,\ \left(\bar{\mu}_{\bar{\mathcal{A}}_t} + \bar{\mu}_{\bar{\mathcal{B}}_t}\right) + \left(\sigma_{\bar{\mathcal{A}}_t} + \sigma_{\bar{\mathcal{B}}_t}\right)\sqrt{-2\log\alpha}\right]$11(a)

$\bar{\bar{\mathcal{A}}}_{GN_{it\alpha}} + \bar{\bar{\mathcal{B}}}_{GN_{it\alpha}} = \left[\left(\bar{\mu}_{\bar{\mathcal{A}}_{it}} + \bar{\mu}_{\bar{\mathcal{B}}_{it}}\right) - \left(\sigma_{\bar{\mathcal{A}}_{it}} + \sigma_{\bar{\mathcal{B}}_{it}}\right)\sqrt{-2\log\alpha}\ ,\ \left(\bar{\mu}_{\bar{\mathcal{A}}_{it}} + \bar{\mu}_{\bar{\mathcal{B}}_{it}}\right) + \left(\sigma_{\bar{\mathcal{A}}_{it}} + \sigma_{\bar{\mathcal{B}}_{it}}\right)\sqrt{-2\log\alpha}\right]$ 11(b)

$\bar{\bar{\mathcal{A}}}_{GN_{if\alpha}} + \bar{\bar{\mathcal{B}}}_{GN_{if\alpha}} = \left[\left(\bar{\mu}_{\bar{\mathcal{A}}_{if}} + \bar{\mu}_{\bar{\mathcal{B}}_{if}}\right) - \left(\sigma_{\bar{\mathcal{A}}_{if}} + \sigma_{\bar{\mathcal{B}}_{if}}\right)\sqrt{-2\log(1-\alpha)}\ ,\ \left(\bar{\mu}_{\bar{\mathcal{A}}_{if}} + \bar{\mu}_{\bar{\mathcal{B}}_{if}}\right) + \left(\sigma_{\bar{\mathcal{A}}_{if}} + \sigma_{\bar{\mathcal{B}}_{if}}\right)\sqrt{-2\log(1-\alpha)}\right]$ 11(c)

$\bar{\bar{\mathcal{A}}}_{GN_{f\alpha}} + \bar{\bar{\mathcal{B}}}_{GN_{f\alpha}} = \left[\left(\bar{\mu}_{\bar{\mathcal{A}}_f} + \bar{\mu}_{\bar{\mathcal{B}}_f}\right) - \left(\sigma_{\bar{\mathcal{A}}_f} + \sigma_{\bar{\mathcal{B}}_f}\right)\sqrt{-2\log(1-\alpha)}\ ,\ \left(\bar{\mu}_{\bar{\mathcal{A}}_f} + \bar{\mu}_{\bar{\mathcal{B}}_f}\right) + \left(\sigma_{\bar{\mathcal{A}}_f} + \sigma_{\bar{\mathcal{B}}_f}\right)\sqrt{-2\log(1-\alpha)}\right]$ 11(d)

Truth membership function, indeterminacy leaning towards truth membership function, indeterminacy leaning towards falsity membership function and falsity membership function of addition of Gaussian Double Refined Indeterminate Neutrosophic Numbers $\bar{\bar{\mathcal{A}}}_{GN}$ and $\bar{\bar{\mathcal{B}}}_{GN}$are as follows.

$\psi_{(\bar{\bar{\mathcal{A}}}_{GN}+\bar{\bar{\mathcal{B}}}_{GN})}(x_t) = \exp\left(-\frac{1}{2}\left(\frac{x_t-\left(\bar{\mu}_{\bar{\mathcal{A}}_t}+\bar{\mu}_{\bar{\mathcal{B}}_t}\right)}{\sigma_{\bar{\mathcal{A}}_t}+\sigma_{\bar{\mathcal{B}}_t}}\right)^2\right)$ 12(a)

$$\psi_{(\bar{\bar{\mathcal{A}}}_{GN}+\bar{\bar{\mathcal{B}}}_{GN})}(x_{it}) = \exp\left(-\frac{1}{2}\left(\frac{x_{it}-\left(\bar{\mu}_{\bar{\bar{\mathcal{A}}}_{it}}+\bar{\mu}_{\bar{\bar{\mathcal{B}}}_{it}}\right)}{\sigma_{\bar{\bar{\mathcal{A}}}_{it}}+\sigma_{\bar{\bar{\mathcal{B}}}_{it}}}\right)^2\right) \quad 12(b)$$

$$\psi_{(\bar{\bar{\mathcal{A}}}_{GN}+\bar{\bar{\mathcal{B}}}_{GN})}(x_{if}) = 1 - \exp\left(-\frac{1}{2}\left(\frac{x_{if}-\left(\bar{\mu}_{\bar{\bar{\mathcal{A}}}_{if}}+\bar{\mu}_{\bar{\bar{\mathcal{B}}}_{if}}\right)}{\sigma_{\bar{\bar{\mathcal{A}}}_{if}}+\sigma_{\bar{\bar{\mathcal{B}}}_{if}}}\right)^2\right) \quad 12(c)$$

$$\psi_{(\bar{\bar{\mathcal{A}}}_{GN}+\bar{\bar{\mathcal{B}}}_{GN})}(x_{f}) = 1 - \exp\left(-\frac{1}{2}\left(\frac{x_{f}-\left(\bar{\mu}_{\bar{\bar{\mathcal{A}}}_{f}}+\bar{\mu}_{\bar{\bar{\mathcal{B}}}_{f}}\right)}{\sigma_{\bar{\bar{\mathcal{A}}}_{f}}+\sigma_{\bar{\bar{\mathcal{B}}}_{f}}}\right)^2\right) \quad 12(d)$$

respectively.

2. Subtraction:

$\bar{\bar{\mathcal{A}}}_{GN_{t\alpha}} - \bar{\bar{\mathcal{B}}}_{GN_{t\alpha}} = \left[\left(\bar{\mu}_{\bar{\bar{\mathcal{A}}}_t} - \bar{\mu}_{\bar{\bar{\mathcal{B}}}_t}\right) - \left(\sigma_{\bar{\bar{\mathcal{A}}}_t} + \sigma_{\bar{\bar{\mathcal{B}}}_t}\right)\sqrt{-2\log\alpha}\,,\ \left(\bar{\mu}_{\bar{\bar{\mathcal{A}}}_t} - \bar{\mu}_{\bar{\bar{\mathcal{B}}}_t}\right) + \left(\sigma_{\bar{\bar{\mathcal{A}}}_t} + \sigma_{\bar{\bar{\mathcal{B}}}_t}\right)\sqrt{-2\log\alpha}\right]$ 13(a)

$\bar{\bar{\mathcal{A}}}_{GN_{it\alpha}} - \bar{\bar{\mathcal{B}}}_{GN_{it\alpha}} = \left[\left(\bar{\mu}_{\bar{\bar{\mathcal{A}}}_{it}} - \bar{\mu}_{\bar{\bar{\mathcal{B}}}_{it}}\right) - \left(\sigma_{\bar{\bar{\mathcal{A}}}_{it}} + \sigma_{\bar{\bar{\mathcal{B}}}_{it}}\right)\sqrt{-2\log\alpha}\,,\ \left(\bar{\mu}_{\bar{\bar{\mathcal{A}}}_{it}} - \bar{\mu}_{\bar{\bar{\mathcal{B}}}_{it}}\right) + \left(\sigma_{\bar{\bar{\mathcal{A}}}_{it}} + \sigma_{\bar{\bar{\mathcal{B}}}_{it}}\right)\sqrt{-2\log\alpha}\right]$ 13(b)

$\bar{\bar{\mathcal{A}}}_{GN_{if\alpha}} - \bar{\bar{\mathcal{B}}}_{GN_{if\alpha}} = \left[\left(\bar{\mu}_{\bar{\bar{\mathcal{A}}}_{if}} - \bar{\mu}_{\bar{\bar{\mathcal{B}}}_{if}}\right) - \left(\sigma_{\bar{\bar{\mathcal{A}}}_{if}} + \sigma_{\bar{\bar{\mathcal{B}}}_{if}}\right)\sqrt{-2\log(1-\alpha)}\,,\ \left(\bar{\mu}_{\bar{\bar{\mathcal{A}}}_{if}} - \bar{\mu}_{\bar{\bar{\mathcal{B}}}_{if}}\right) + \left(\sigma_{\bar{\bar{\mathcal{A}}}_{if}} + \sigma_{\bar{\bar{\mathcal{B}}}_{if}}\right)\sqrt{-2\log(1-\alpha)}\right]$ 13(c)

$\bar{\bar{\mathcal{A}}}_{GN_{f\alpha}} - \bar{\bar{\mathcal{B}}}_{GN_{f\alpha}} = \left[\left(\bar{\mu}_{\bar{\bar{\mathcal{A}}}_{f}} - \bar{\mu}_{\bar{\bar{\mathcal{B}}}_{f}}\right) - \left(\sigma_{\bar{\bar{\mathcal{A}}}_{f}} + \sigma_{\bar{\bar{\mathcal{B}}}_{f}}\right)\sqrt{-2\log(1-\alpha)}\,,\ \left(\bar{\mu}_{\bar{\bar{\mathcal{A}}}_{f}} - \bar{\mu}_{\bar{\bar{\mathcal{B}}}_{f}}\right) + \left(\sigma_{\bar{\bar{\mathcal{A}}}_{f}} + \sigma_{\bar{\bar{\mathcal{B}}}_{f}}\right)\sqrt{-2\log(1-\alpha)}\right]$ 13(d)

Truth membership function, indeterminacy leaning towards truth membership function, indeterminacy leaning towards falsity membership function and falsity membership function of subtraction of Gaussian Double Refined Indeterminate Neutrosophic Numbers $\bar{\bar{\mathcal{A}}}_{GN}$ and $\bar{\bar{\mathcal{B}}}_{GN}$ are as follows.

$$\psi_{(\bar{\bar{\mathcal{A}}}_{GN}-\bar{\bar{\mathcal{B}}}_{GN})}(x_{t}) = \exp\left(-\frac{1}{2}\left(\frac{x_{t}-\left(\bar{\mu}_{\bar{\bar{\mathcal{A}}}_{t}}-\bar{\mu}_{\bar{\bar{\mathcal{B}}}_{t}}\right)}{\sigma_{\bar{\bar{\mathcal{A}}}_{t}}+\sigma_{\bar{\bar{\mathcal{B}}}_{t}}}\right)^2\right) \quad 14(a)$$

$$\psi_{(\bar{\bar{\mathcal{A}}}_{GN}-\bar{\bar{\mathcal{B}}}_{GN})}(x_{it}) = \exp\left(-\frac{1}{2}\left(\frac{x_{it}-\left(\bar{\mu}_{\bar{\bar{\mathcal{A}}}_{it}}-\bar{\mu}_{\bar{\bar{\mathcal{B}}}_{it}}\right)}{\sigma_{\bar{\bar{\mathcal{A}}}_{it}}+\sigma_{\bar{\bar{\mathcal{B}}}_{it}}}\right)^2\right) \quad 14(b)$$

$$\psi_{(\bar{\bar{\mathcal{A}}}_{GN}-\bar{\bar{\mathcal{B}}}_{GN})}(x_{if}) = 1 - \exp\left(-\frac{1}{2}\left(\frac{x_{if}-\left(\bar{\mu}_{\bar{\bar{\mathcal{A}}}_{if}}-\bar{\mu}_{\bar{\bar{\mathcal{B}}}_{if}}\right)}{\sigma_{\bar{\bar{\mathcal{A}}}_{if}}+\sigma_{\bar{\bar{\mathcal{B}}}_{if}}}\right)^2\right) \quad 14(c)$$

and

$$\psi_{(\bar{\bar{\mathcal{A}}}_{GN}-\bar{\bar{\mathcal{B}}}_{GN})}(x_{f}) = 1 - \exp\left(-\frac{1}{2}\left(\frac{x_{f}-\left(\bar{\mu}_{\bar{\bar{\mathcal{A}}}_{f}}-\bar{\mu}_{\bar{\bar{\mathcal{B}}}_{f}}\right)}{\sigma_{\bar{\bar{\mathcal{A}}}_{f}}+\sigma_{\bar{\bar{\mathcal{B}}}_{f}}}\right)^2\right) \quad 14(d)$$

3.Multiplication:

$\bar{\bar{\mathcal{A}}}_{GN_{t\alpha}} \cdot \bar{\bar{\mathcal{B}}}_{GN_{t\alpha}} = \left[\left(\bar{\mu}_{\bar{\bar{\mathcal{A}}}_t} - \sigma_{\bar{\bar{\mathcal{A}}}_t}\sqrt{-2\log\alpha}\right) \cdot \left(\bar{\mu}_{\bar{\bar{\mathcal{B}}}_t} - \sigma_{\bar{\bar{\mathcal{B}}}_t}\sqrt{-2\log\alpha}\right),\ \left(\bar{\mu}_{\bar{\bar{\mathcal{A}}}_t} + \sigma_{\bar{\bar{\mathcal{A}}}_t}\sqrt{-2\log\alpha}\right) \cdot \left(\bar{\mu}_{\bar{\bar{\mathcal{B}}}_t} + \sigma_{\bar{\bar{\mathcal{B}}}_t}\sqrt{-2\log\alpha}\right)\right]$ 15(a)

$\bar{\bar{\mathcal{A}}}_{GN_{it\alpha}} \cdot \bar{\bar{\mathcal{B}}}_{GN_{it\alpha}} = \left[\left(\bar{\mu}_{\bar{\bar{\mathcal{A}}}_{it}} - \sigma_{\bar{\bar{\mathcal{A}}}_{it}}\sqrt{-2\log\alpha}\right) \cdot \left(\bar{\mu}_{\bar{\bar{\mathcal{B}}}_{it}} - \sigma_{\bar{\bar{\mathcal{B}}}_{it}}\sqrt{-2\log\alpha}\right),\ \left(\bar{\mu}_{\bar{\bar{\mathcal{A}}}_{it}} + \sigma_{\bar{\bar{\mathcal{A}}}_{it}}\sqrt{-2\log\alpha}\right) \cdot \left(\bar{\mu}_{\bar{\bar{\mathcal{B}}}_{it}} + \sigma_{\bar{\bar{\mathcal{B}}}_{it}}\sqrt{-2\log\alpha}\right)\right]$ 15(b)

$\bar{\bar{\mathcal{A}}}_{GN_{if\alpha}} \cdot \bar{\bar{\mathcal{B}}}_{GN_{if\alpha}} = \left[\left(\bar{\mu}_{\bar{\bar{\mathcal{A}}}_{if}} - \sigma_{\bar{\bar{\mathcal{A}}}_{if}}\sqrt{-2\log(1-\alpha)}\right) \cdot \left(\bar{\mu}_{\bar{\bar{\mathcal{B}}}_{if}} - \sigma_{\bar{\bar{\mathcal{B}}}_{if}}\sqrt{-2\log(1-\alpha)}\right),\ \left(\bar{\mu}_{\bar{\bar{\mathcal{A}}}_{if}} + \sigma_{\bar{\bar{\mathcal{A}}}_{if}}\sqrt{-2\log(1-\alpha)}\right) \cdot \left(\bar{\mu}_{\bar{\bar{\mathcal{B}}}_{if}} + \sigma_{\bar{\bar{\mathcal{B}}}_{if}}\sqrt{-2\log(1-\alpha)}\right)\right]$ 15(c)

$$\bar{\bar{\mathcal{A}}}_{GN_{f\alpha}} \cdot \bar{\bar{\mathcal{B}}}_{GN_{f\alpha}} = \left[\left(\bar{\mu}_{\bar{\mathcal{A}}_f} - \sigma_{\bar{\mathcal{A}}_f}\sqrt{-2\log(1-\alpha)}\right) \cdot \left(\bar{\mu}_{\bar{\bar{\mathcal{B}}}_f} - \sigma_{\bar{\bar{\mathcal{B}}}_f}\sqrt{-2\log(1-\alpha)}\right), \left(\bar{\mu}_{\bar{\mathcal{A}}_f} + \sigma_{\bar{\bar{\mathcal{A}}}_f}\sqrt{-2\log(1-\alpha)}\right) \cdot \left(\bar{\mu}_{\bar{\bar{\mathcal{B}}}_f} + \sigma_{\bar{\bar{\mathcal{B}}}_f}\sqrt{-2\log(1-\alpha)}\right)\right]$$

15(d)

4. Division:

$$\frac{\bar{\mathcal{A}}_{GN_{t\alpha}}}{\bar{\bar{\mathcal{B}}}_{GN_{t\alpha}}} = \left[\frac{\bar{\mu}_{\bar{\mathcal{A}}_t} - \sigma_{\bar{\mathcal{A}}_t}\sqrt{-2\log\alpha}}{\bar{\mu}_{\bar{\bar{\mathcal{B}}}_t} + \sigma_{\bar{\bar{\mathcal{B}}}_t}\sqrt{-2\log\alpha}}, \frac{\bar{\mu}_{\bar{\mathcal{A}}_t} + \sigma_{\bar{\mathcal{A}}_t}\sqrt{-2\log\alpha}}{\bar{\mu}_{\bar{\bar{\mathcal{B}}}_t} - \sigma_{\bar{\bar{\mathcal{B}}}_t}\sqrt{-2\log\alpha}}\right] \quad 16(a)$$

$$\frac{\bar{\mathcal{A}}_{GN_{it\alpha}}}{\bar{\bar{\mathcal{B}}}_{GN_{it\alpha}}} = \left[\frac{\bar{\mu}_{\bar{\mathcal{A}}_{it}} - \sigma_{\bar{\mathcal{A}}_{it}}\sqrt{-2\log\alpha}}{\bar{\mu}_{\bar{\bar{\mathcal{B}}}_{it}} + \sigma_{\bar{\bar{\mathcal{B}}}_{it}}\sqrt{-2\log\alpha}}, \frac{\bar{\mu}_{\bar{\mathcal{A}}_{it}} + \sigma_{\bar{\bar{\mathcal{A}}}_{it}}\sqrt{-2\log\alpha}}{\bar{\mu}_{\bar{\bar{\mathcal{B}}}_{it}} - \sigma_{\bar{\bar{\mathcal{B}}}_{it}}\sqrt{-2\log\alpha}}\right] \quad 16(b)$$

$$\frac{\bar{\mathcal{A}}_{GN_{if\alpha}}}{\bar{\bar{\mathcal{B}}}_{GN_{if\alpha}}} = \left[\frac{\bar{\mu}_{\bar{\mathcal{A}}_{if}} - \sigma_{\bar{\mathcal{A}}_{if}}\sqrt{-2\log(1-\alpha)}}{\bar{\mu}_{\bar{\bar{\mathcal{B}}}_{if}} + \sigma_{\bar{\bar{\mathcal{B}}}_{if}}\sqrt{-2\log(1-\alpha)}}, \frac{\bar{\mu}_{\bar{\mathcal{A}}_{if}} + \sigma_{\bar{\bar{\mathcal{A}}}_{if}}\sqrt{-2\log(1-\alpha)}}{\bar{\mu}_{\bar{\bar{\mathcal{B}}}_{if}} - \sigma_{\bar{\bar{\mathcal{B}}}_{if}}\sqrt{-2\log(1-\alpha)}}\right] \quad 16(c)$$

$$\frac{\bar{\mathcal{A}}_{GN_{f\alpha}}}{\bar{\bar{\mathcal{B}}}_{GN_{f\alpha}}} = \left[\frac{\bar{\mu}_{\bar{\mathcal{A}}_f} - \sigma_{\bar{\mathcal{A}}_f}\sqrt{-2\log(1-\alpha)}}{\bar{\mu}_{\bar{\bar{\mathcal{B}}}_f} - \sigma_{\bar{\bar{\mathcal{B}}}_f}\sqrt{-2\log(1-\alpha)}}, \frac{\bar{\mu}_{\bar{\mathcal{A}}_f} + \sigma_{\bar{\bar{\mathcal{A}}}_f}\sqrt{-2\log(1-\alpha)}}{\bar{\mu}_{\bar{\bar{\mathcal{B}}}_f} + \sigma_{\bar{\bar{\mathcal{B}}}_f}\sqrt{-2\log(1-\alpha)}}\right] 16(d)$$

The Gaussian function applied to image help distinguish edge pixel excepted from clustering process. Using the cluster centres obtained image are segmented and exported to local memory for the image. By using the GBTDRINSS, the image segmentation process of image is achieved by using the procedure of finding the edges of image using positive degree of indeterminate member pixel.

3.3 Transforming the image into NSS

3.3.1 Neutroscophic Image (NI):

Let V be the universe of the discourse and the image window $\mathcal{W} = w * w$, i.e., rows and columns in spatial domain. Thus, $\mathcal{W}$ is a collection of image intensity pixels, where $\mathcal{W} \subseteq$ V and it holds with bright pixels. As per the Eq. (17), the NI is generally characterized by the three membership sets T, I and F. For the collected image, the dimensions of A^*B with each pixels$P = (a, b)$ is represented as $P_{NS}(a, b)$ in the image.

$$T(a,b) = \frac{\overline{g(a,b)} - \overline{g_{min}}}{\overline{g_{max}} - \overline{g_{min}}} (18)$$

$$\overline{g(a,b)} = \frac{1}{w*w}\sum_{k=a-w/2}^{a+w/2}\sum_{l=b-w/2}^{b+w/2} g(k,l) (19)$$

$$I(a,b) = \frac{\delta(a,b) - \delta_{min}}{\delta_{min} - \delta_{min}} \quad (20)$$

$$\delta(a,b) = abs(g(a,b) - \overline{g(a,b)}) (21)$$

$$F(a,b) = 1 - T(a,b) \quad (22)$$

$P_{NS}(a, b) = \{T(a, b), I(a, b), F(a, b)\}$(17)

In Eq. (17), $P_{NS}(a, b)$ interpret the memberships to bright, indeterminate and black intensity values through true $T(a, b)$, indeterminate $I(a, b)$ and False $F(a, b)$ which is represented in the following Eqs. (18-22),

Where, $g(a, b)$ is the intensity value of the pixel (a, b), $\overline{g(a, b)}$ is the local mean value of $g(a, b)$, $\delta(a, b)$ is the absolute value of the difference between intensity $g(a, b)$ and its local mean value $\overline{g(a, b)}$.

3.3.2 Bipolar Trapezoidal Double Refined Indeterminate Neutrosophic Image (BTDRINI)

BTDRINI is generally characterized by the various polarity membership sets like truth membership (p_{B_iT}), indeterminacy leaning towards truth membership (q_{B_iT}), indeterminacy leaning towards falsity membership (r_{B_iT}) and falsity membership (s_{B_iT}) to transform the gray scale image to BTDRINSS. For the collected image, the pixel in BTDRINSS is represented as $\ddot{\mathcal{A}}_{B_iT}$which is depicted in Eq. (23).,

$$\ddot{\mathcal{A}}_{B_iT} = \left(a_1, a_2, a_3, a_4 ; p_{B_iT}, q_{B_iT}, r_{B_iT}, s_{B_iT}\right) (23)$$

In Eq. (23),$\ddot{\mathcal{A}}_{B_iT}$interpret the BTDRINImemberships to $T^+(x)$, $T^-(x))$, ${I_T}^+(x)$, ${I_T}^-(x)$, ${I_F}^+(x)$, ${I_F}^-(x)$, $F^+(x)$and $F^-(x)$which is represented in the table 2, following Eqs. (24(a-h)). a_1, a_2, a_3, a_4 represents the mean intensity of foreground pixel in element x.

Table 2 Positive and Negative Degree Membership's in BTDRINSS

Positive Degree of Truth-Membership	**Negative Degree of Truth-Membership**
$T^{+}(x)=\begin{cases} p_{B_iT}\frac{x-a_1}{a_2-a_1}a_1 \le x < a_2 \\ p_{B_iT}a_2 \le x \le a_3 \\ p_{B_iT}\frac{a_4-x}{a_4-a_3}a_3 < x \le a_4 \\ 0 \quad otherwise \end{cases}$ (24(a))	$T^{-}(x)=\begin{cases} p_{B_iT}\frac{a_1-x}{a_2-a_1}a_1 \le x < a_2 \\ -p_{B_iT}a_2 \le x \le a_3 \\ p_{B_iT}\frac{x-a_4}{a_4-a_3}a_3 < x \le a_4 \\ 0 \quad otherwise \end{cases}$ (24(b))
Positive degree of Indeterminate toward Truth Membership	**Negative degree of indeterminate towards truth membership**
$I_T{}^{+}(x)=\begin{cases} q_{B_iT}\frac{x-a_1}{a_2-a_1}a_1 \le x < a_2 \\ q_{B_iT}a_2 \le x \le a_3 \\ q_{B_iT}\frac{a_4-x}{a_4-a_3}a_3 < x \le a_4 \\ 0 \quad otherwise \end{cases}$ (24(c))	$I_T{}^{-}(x)=\begin{cases} q_{B_iT}\frac{a_1-x}{a_2-a_1}a_1 \le x < a_2 \\ -q_{B_iT}a_2 \le x \le a_3 \\ q_{B_iT}\frac{x-a_4}{a_4-a_3}a_3 < x \le a_4 \\ 0 \quad otherwise \end{cases}$ (24(d))
Positive Degree of Indeterminate toward Falsity membership	**Negative Degree of Indeterminate toward Falsity membership**
$I_F{}^{+}(x)=\begin{cases} \frac{a_2-x+r_{B_iT}(x-a_1)}{a_2-a_1}a_1 \le x < a_2 \\ r_{B_iT}a_2 \le x \le a_3 \\ \frac{x-a_3+r_{B_iT}(a_4-x)}{a_4-a_3}a_3 < x \le a_4 \\ 1 \quad otherwise \end{cases}$ (24(e))	$I_F{}^{-}(x)=\begin{cases} \frac{x-a_2+r_{B_iT}(a_1-x)}{a_2-a_1}a_1 \le x < a_2 \\ -r_{B_iT}a_2 \le x \le a_3 \\ \frac{a_3-x+r_{B_iT}(x-a_4)}{a_4-a_3}a_3 < x \le a_4 \\ -1 \quad otherwise \end{cases}$ (24(f))
Positive degree of Falsity membership	**Negative degree of Falsity membership**
$F^{+}(x)=\begin{cases} \frac{a_2-x+s_{B_iT}(x-a_1)}{a_2-a_1}a_1 \le x < a_2 \\ s_{B_iT}a_2 \le x \le a_3 \\ \frac{x-a_3+s_{B_iT}(a_4-x)}{a_4-a_3}a_3 < x \le a_4 \\ 1 \quad otherwise \end{cases}$ (24(g))	$F^{-}(x)=\begin{cases} \frac{x-a_2+s_{B_iT}(a_1-x)}{a_2-a_1}a_1 \le x < a_2 \\ -s_{B_iT}a_2 \le x \le a_3 \\ \frac{a_3-x+s_{B_iT}(x-a_4)}{a_4-a_3}a_3 < x \le a_4 \\ -1 \quad otherwise \end{cases}$ (24(h))

3.3.3 Gaussian Bipolar Trapezoidal Double Refined Indeterminate Neutrosophic Image (GBTDRINI)

GBTDRINSS is generally characterized by the mean and SD of truth membership function, indeterminacy leaning towards truth membership function, indeterminacy leaning towards falsity membership function and falsity membership function under two domain sets of GBTDRINSS of Eq. (25) and (26) i.e.,

$$\bar{\bar{\mathcal{A}}}_{GN}=\left(\bar{\mu}_{\bar{\mathcal{A}}_t},\sigma_{\bar{\mathcal{A}}_t}\right),\left(\bar{\mu}_{\bar{\mathcal{A}}_{it}},\sigma_{\bar{\mathcal{A}}_{it}}\right),\left(\bar{\mu}_{\bar{\mathcal{A}}_{if}},\sigma_{\bar{\mathcal{A}}_{if}}\right),\left(\bar{\mu}_{\bar{\mathcal{A}}_f},\sigma_{\bar{\mathcal{A}}_f}\right) \quad (25)$$

and

$$\bar{\bar{\mathcal{B}}}_{GN}=\left(\bar{\mu}_{\bar{\mathcal{B}}_t},\sigma_{\bar{\mathcal{B}}_t}\right),\left(\bar{\mu}_{\bar{\mathcal{B}}_{it}},\sigma_{\bar{\mathcal{B}}_{it}}\right),\left(\bar{\mu}_{\bar{\mathcal{B}}_{if}},\sigma_{\bar{\mathcal{B}}_{if}}\right),\left(\bar{\mu}_{\bar{\mathcal{B}}_f},\sigma_{\bar{\mathcal{B}}_f}\right) \quad (26)$$

$\bar{\bar{\mathcal{A}}}_{GN}$ and $\bar{\bar{\mathcal{B}}}_{GN}$ interprets the intensity values through the truth membership function $t(\bar{\bar{\mathcal{A}}}_{GN},\bar{\bar{\mathcal{B}}}_{GN})$ $(i_t(\bar{\bar{\mathcal{A}}}_{GN},\bar{\bar{\mathcal{B}}}_{GN}))$ and falsity membership function $(f(\bar{\bar{\mathcal{A}}}_{GN},\bar{\bar{\mathcal{B}}}_{GN}))$ which is represented in indeterminacy leaning towards truth membership function $(i_t(\bar{\bar{\mathcal{A}}}_{GN},\bar{\bar{\mathcal{B}}}_{GN}))$, indeterminacy leaning towards falsity membership function Eq. (27(a-d))

$$t(\bar{\bar{\mathcal{A}}}_{GN},\bar{\bar{\mathcal{B}}}_{GN})==\frac{g(\bar{\bar{\mathcal{A}}}_{GN},\bar{\bar{\mathcal{B}}}_{GN})-\left(\left(\bar{\mu}_{\bar{\mathcal{A}}_t}+\bar{\mu}_{\bar{\mathcal{B}}_t}\right)-\left(\sigma_{\bar{\mathcal{A}}_t}+\sigma_{\bar{\mathcal{B}}_t}\right)\sqrt{-2\log\alpha}\right)}{\left(\left(\bar{\mu}_{\bar{\mathcal{A}}_t}+\bar{\mu}_{\bar{\mathcal{B}}_t}\right)-\left(\sigma_{\bar{\mathcal{A}}_t}+\sigma_{\bar{\mathcal{B}}_t}\right)\sqrt{-2\log\alpha}\right)-\left(\left(\bar{\mu}_{\bar{\mathcal{A}}_t}+\bar{\mu}_{\bar{\mathcal{B}}_t}\right)+\left(\sigma_{\bar{\mathcal{A}}_t}+\sigma_{\bar{\mathcal{B}}_t}\right)\sqrt{-2\log\alpha}\right)} \quad (27(a))$$

$$i_t(\bar{\bar{\mathcal{A}}}_{GN},\bar{\bar{\mathcal{B}}}_{GN})==\frac{\left(\left(\bar{\mu}_{\bar{\mathcal{A}}_t},\sigma_{\bar{\mathcal{A}}_t}\right),\left(\bar{\mu}_{\bar{\mathcal{B}}_t},\sigma_{\bar{\mathcal{B}}_t}\right)\right)-\left(\left(\bar{\mu}_{\bar{\mathcal{A}}_{if}}+\bar{\mu}_{\bar{\mathcal{B}}_{if}}\right)-\left(\sigma_{\bar{\mathcal{A}}_{if}}+\sigma_{\bar{\mathcal{B}}_{if}}\right)\sqrt{-2\log(1-\alpha)}\right)}{\left(\left(\bar{\mu}_{\bar{\mathcal{A}}_{it}}+\bar{\mu}_{\bar{\mathcal{B}}_{it}}\right)-\left(\sigma_{\bar{\mathcal{A}}_{it}}+\sigma_{\bar{\mathcal{B}}_{it}}\right)\sqrt{-2\log\alpha}\right)-\left(\left(\bar{\mu}_{\bar{\mathcal{A}}_{it}}+\bar{\mu}_{\bar{\mathcal{B}}_{it}}\right)+\left(\sigma_{\bar{\mathcal{A}}_{it}}+\sigma_{\bar{\mathcal{B}}_{it}}\right)\sqrt{-2\log\alpha}\right)} \quad (27(b))$$

$$i_f(\bar{\bar{\mathcal{A}}}_{GN},\bar{\bar{\mathcal{B}}}_{GN})=\frac{\left(\left(\bar{\mu}_{\bar{\mathcal{A}}_{it}},\sigma_{\bar{\mathcal{A}}_{if}}\right),\left(\bar{\mu}_{\bar{\mathcal{B}}_{if}},\sigma_{\bar{\mathcal{B}}_{if}}\right)\right)-\left(\left(\bar{\mu}_{\bar{\mathcal{A}}_{if}}+\bar{\mu}_{\bar{\mathcal{B}}_{if}}\right)-\left(\sigma_{\bar{\mathcal{A}}_{if}}+\sigma_{\bar{\mathcal{B}}_{if}}\right)\sqrt{-2\log(1-\alpha)}\right)}{\left(\left(\bar{\mu}_{\bar{\mathcal{A}}_{if}}+\bar{\mu}_{\bar{\mathcal{B}}_{if}}\right)-\left(\sigma_{\bar{\mathcal{A}}_{if}}+\sigma_{\bar{\mathcal{B}}_{if}}\right)\sqrt{-2\log\alpha}\right)-\left(\left(\bar{\mu}_{\bar{\mathcal{A}}_{if}}+\bar{\mu}_{\bar{\mathcal{B}}_{if}}\right)+\left(\sigma_{\bar{\mathcal{A}}_{if}}+\sigma_{\bar{\mathcal{B}}_{if}}\right)\sqrt{-2\log\alpha}\right)} \quad (27(c))$$

$$f(\bar{\bar{\mathcal{A}}}_{GN},\bar{\bar{\mathcal{B}}}_{GN})=\frac{(\left(\bar{\mu}_{\bar{\mathcal{A}}_f},\sigma_{\bar{\mathcal{A}}_f}\right),\left(\bar{\mu}_{\bar{\mathcal{B}}_f},\sigma_{\bar{\mathcal{B}}_f}\right))-(\left(\bar{\mu}_{\bar{\mathcal{A}}_f}+\bar{\mu}_{\bar{\mathcal{B}}_f}\right)-\left(\sigma_{\bar{\mathcal{A}}_f}+\sigma_{\bar{\mathcal{B}}_f}\right)\sqrt{-2\log(1-\alpha)})}{\left(\left(\bar{\mu}_{\bar{\mathcal{A}}_f}+\bar{\mu}_{\bar{\mathcal{B}}_f}\right)-\left(\sigma_{\bar{\mathcal{A}}_f}+\sigma_{\bar{\mathcal{B}}_f}\right)\sqrt{-2\log\alpha}\right)-(\left(\bar{\mu}_{\bar{\mathcal{A}}_f}+\bar{\mu}_{\bar{\mathcal{B}}_f}\right)+\left(\sigma_{\bar{\mathcal{A}}_f}+\sigma_{\bar{\mathcal{B}}_f}\right)\sqrt{-2\log\alpha})} \quad (27(d))$$

The above mentioned GBTDRINI are based on the σ and μ, the $\bar{\bar{\mathcal{A}}}_t$, $\bar{\bar{\mathcal{A}}}_{it}$, $\bar{\bar{\mathcal{A}}}_{if}$, $\bar{\bar{\mathcal{A}}}_f$ and $\bar{\bar{\mathcal{B}}}_t$, $\bar{\bar{\mathcal{B}}}_{it}$, $\bar{\bar{\mathcal{B}}}_{if}$, $\bar{\bar{\mathcal{B}}}_f$ will be the GBTDRINI membership values in GBTDRINSS domain.

3.4 Image Entropy in NS domain

3.4.1 Neutrosophic Image (NI) entropy

For a gray level image, the entropy evaluates the distribution of the intensities. If the entropy is maximum, the intensities have equal probability and they distribute uniformly. If the entropy is small, the intensities have different probabilities and their distributions are non-uniform. The NI entropy is defined as the summation of the entropies of three sets T, I and F which is employed to determine the distribution of the elements in the neutrosophic domain which is illustrated in following Eqs. (28- 29(c))

$$E_{NS}=E_T+E_I+E_F \quad (28)$$

$$E_T=-\sum_{a=\min\{T\}}^{\max\{T\}}P_T(a)lnP_T(a) \quad (29(a))$$

$$E_I=-\sum_{a=\min\{I\}}^{\max\{I\}}P_I(a)lnP_I(a) \quad (29(b))$$

$$E_F=-\sum_{a=\min\{F\}}^{\max\{F\}}P_F(a)lnP_F(a) \quad (29(c))$$

Where, E_T, E_I and E_F are the entropies of the sets T, I and F respectively and $P_T(a)$, $P_I(a)$ and$P_F(a)$ are the probabilities of the elements in T, I and F respectively.

3.4.2BTDRINI ENTROPY

The same condition in NI entropy is followed BTDRINSS domainThe BTDRINI Entropy defined as sum of entropies of all subsets T^+, T^-, ${I_T}^+$, ${I_T}^-$, ${I_F}^+$, ${I_F}^-$, F^+ and F^-which is used to determine the distribution of pixels in BTDRINSSdomain.

$$E_{BTDRINS}=E_{T^+}+E_{T^-}+E_{{I_T}^+}+E_{{I_T}^-}+E_{{I_F}^+}+E_{{I_F}^-}+E_{F^+}+E_{F^-} \quad (30)$$

$$E_{T^+}=-\sum_{a=\min\{T^+\}}^{\max\{T^+\}}P_{T^+}(p_{B_iT^+}(a)lnp_{B_iT^+}(a)) \quad 31(a)$$

$$E_{T^-}=-\sum_{a=\min\{T^-\}}^{\max\{T^-\}}P_{T^-}(p_{B_iT^-}(a)lnp_{B_iT^-}(a)) \quad 31(b)$$

$$E_{{I_T}^+}=-\sum_{a=\min\{{I_T}^+\}}^{\max\{{I_T}^+\}}P_{{I_T}^+}(q_{B_i{I_T}^+}(a)lnq_{B_i{I_T}^+}(a)) \quad 31(c)$$

$$E_{{I_T}^-}=-\sum_{a=\min\{{I_T}^-,\}}^{\max\{{I_T}^-\}}P_{{I_T}^-}(q_{B_i{I_T}^-}(a)lnq_{B_i{I_T}^-}(a)) \quad 31(d)$$

$$E_{{I_F}^+}=-\sum_{a=\min\{{I_F}^+\}}^{\max\{{I_F}^+\}}P_{{I_F}^+}(r_{B_i{I_F}^+}(a)lnr_{B_i{I_F}^+}(a)) \quad 31(e)$$

$$E_{{I_F}^-}=-\sum_{a=\min\{{I_F}^-,\}}^{\max\{{I_{TF}}^-\}}P_{{I_F}^-}(r_{B_i{I_F}^-}-(a)lnr_{{I_F}^-}(a)) \quad 31(f)$$

$$E_{F^+}=-\sum_{a=\min\{F^+\}}^{\max\{F^+\}}P_{F^+}(s_{B_iF^-}(a)lns_{B_iF^-}(a)) \quad 31(g)$$

$$E_{F^-}=-\sum_{a=\min\{F^-\}}^{\max\{F^-\}}P_{F^-}(s_{B_iF^-}(a)lns_{B_iF^-}(a)) \quad 31(h)$$

From Eq. (30-31(h)) $E_{T^+}+E_{T^-}+E_{{I_T}^+}+E_{{I_T}^-}+E_{{I_F}^+}+E_{{I_F}^-}+E_{F^+}+E_{F^-}$are the entropies of the positiveand Negative degree membership's in BTDRINSS respectively;P_{T^+} , P_{T^-} , $P_{{I_T}^+}$,$P_{{I_T}^-}$, $P_{{I_F}^+}P_{{I_F}^-}$, P_{F^+} and $P_{F^-}$are the probabilities of the elements inT^+, T^-, ${I_T}^+$, ${I_T}^-$, ${I_F}^+$, ${I_F}^-$, F^+ and F^-respectively.

3.4.3 GBTDRINI ENTROPY

The GBTDRINI Entropy defined as sum of entropies of all subsets $\bar{\bar{\mathcal{A}}}_t$, $\bar{\bar{\mathcal{A}}}_{it}$, $\bar{\bar{\mathcal{A}}}_{if}$, $\bar{\bar{\mathcal{A}}}_f$ and $\bar{\bar{\mathcal{B}}}_t$, $\bar{\bar{\mathcal{B}}}_{it}$, $\bar{\bar{\mathcal{B}}}_{if}$, $\bar{\bar{\mathcal{B}}}_f$ which is used to determine the distribution of pixels in GBTDRINI. The entropies of two domain GBTDRINI are equated in Eq. (32) and (33).,

$$E_{\bar{\bar{\mathcal{A}}}_{GN}}=E_{\bar{\bar{\mathcal{A}}}_t}+E_{\bar{\bar{\mathcal{A}}}_{it}}+E_{\bar{\bar{\mathcal{A}}}_{if}}+E_{\bar{\bar{\mathcal{A}}}_f} \quad (32)$$

$$E_{\bar{\bar{\mathcal{B}}}_{GN}}=E_{\bar{\bar{\mathcal{B}}}_t}+E_{\bar{\bar{\mathcal{B}}}_{it}}+E_{\bar{\bar{\mathcal{B}}}_{if}}+E_{\bar{\bar{\mathcal{B}}}_f} \quad (33)$$

Table 3 GBTDRINI Entropy

$E_{\bar{\bar{\mathcal{A}}}_t}=\sum_{a=\min\{\bar{\bar{\mathcal{A}}}_t\}}^{\max\{\bar{\bar{\mathcal{A}}}_t\}}P_{\bar{\bar{\mathcal{A}}}_t}(\bar{\bar{\mathcal{A}}}_t)lnP_{\bar{\bar{\mathcal{A}}}_t}(\bar{\bar{\mathcal{A}}}_t)$ 34(a)	$E_{\bar{\bar{\mathcal{B}}}_t}=\sum_{a=\min\{\bar{\bar{\mathcal{B}}}_t\}}^{\max\{\bar{\bar{\mathcal{B}}}_t\}}P_{\bar{\bar{\mathcal{B}}}_t}(\bar{\bar{\mathcal{B}}}_t)lnP_{\bar{\bar{\mathcal{B}}}_t}(\bar{\bar{\mathcal{B}}}_t)$34(b)
$E_{\bar{\bar{\mathcal{A}}}_{it}}=\sum_{a=\min\{\bar{\bar{\mathcal{A}}}_{it}\}}^{\max\{\bar{\bar{\mathcal{A}}}_{it}\}}P_{\bar{\bar{\mathcal{A}}}_{it}}(\bar{\bar{\mathcal{A}}}_{it})lnP_{\bar{\bar{\mathcal{A}}}_{it}}(\bar{\bar{\mathcal{A}}}_{it})$34(c)	$E_{\bar{\bar{\mathcal{B}}}_{it}}=\sum_{a=\min\{\bar{\bar{\mathcal{A}}}_{it}\}}^{\max\{\bar{\bar{\mathcal{B}}}_{it}\}}P_{\bar{\bar{\mathcal{B}}}_{it}}(\bar{\bar{\mathcal{B}}}_{it})lnP_{\bar{\bar{\mathcal{B}}}_{it}}(\bar{\bar{\mathcal{B}}}_{it})$34(d)

$E_{\bar{\mathcal{A}}_{if}} = \sum_{a=\min\{\bar{\mathcal{A}}_{if}\}}^{\max\{\bar{\mathcal{A}}_{if}\}} P_{\bar{\mathcal{A}}_{if}}(\bar{\mathcal{A}}_{if}) ln P_{\bar{\mathcal{A}}_{if}}(\bar{\mathcal{A}}_{if})$34(e)	$E_{\bar{\bar{B}}_{if}} = \sum_{a=\min\{\bar{\mathcal{A}}_{if}\}}^{\max\{\bar{\bar{B}}_{if}\}} P_{\bar{\bar{B}}_{if}}(\bar{\bar{B}}_{if}) ln P_{\bar{\bar{B}}_{if}}(\bar{\bar{B}}_{if})$34(f)
$E_{\bar{\mathcal{A}}_{f}} = \sum_{a=\min\{\bar{\mathcal{A}}_{f}\}}^{\max\{\bar{\mathcal{A}}_{f}\}} P_{\bar{\mathcal{A}}_{f}}(\bar{\mathcal{A}}_{f}) ln P_{\bar{\mathcal{A}}_{f}}(\bar{\mathcal{A}}_{f})$34(g)	$E_{\bar{\bar{B}}_{f}} = \sum_{a=\min\{\bar{\mathcal{A}}_{f}\}}^{\max\{\bar{\bar{B}}_{f}\}} P_{\bar{\bar{B}}_{f}}(\bar{\bar{B}}_{f}) ln P_{\bar{\bar{B}}_{f}}(\bar{\bar{B}}_{f})$34(h)

Form the above table 3 (Eq. (34(a-h)), $P_{\bar{\mathcal{A}}_t}$,$P_{\bar{\mathcal{A}}_{it}}$, $P_{\bar{\mathcal{A}}_{if}}$, $P_{\bar{\mathcal{A}}_f}$, $P_{\bar{\bar{B}}_t}$, $P_{\bar{\bar{B}}_{it}}$,$P_{\bar{\bar{B}}_{it}}$ and $P_{\bar{\bar{B}}_f}$ are the probabilities of the elements in $\bar{\bar{\mathcal{A}}}_t, \bar{\bar{\mathcal{A}}}_{it}, \bar{\bar{\mathcal{A}}}_{if}, \bar{\bar{\mathcal{A}}}_f$ and $\bar{\bar{\bar{B}}}_t, \bar{\bar{\bar{B}}}_{it}, \bar{\bar{\bar{B}}}_{if}, \bar{\bar{\bar{B}}}_f$ respectively.

3.5 IMAGE PRE-PROCESSING

3.5.1 Pre-processing using NS

The two function like $\alpha - mean$ and$\beta - enhancements$ in NS domain is used for the pre-processing tasks and reduces the indeterminacy of the NI set.

- $\boldsymbol{\alpha - mean}$ **operations**

$$\overline{H(a,b)} = \frac{1}{w*w}\sum_{k=a-w/2}^{a+w/2}\sum_{l=b-w/2}^{b+w/2} H(k,l) \quad (35)$$

The $\alpha - mean$ operation for P_{NS} and $\overline{P_{NS}}$ (α) is defined in Eqs. (36- 41)

$$\overline{P_{NS}}(\alpha) = P\left(\bar{T}(\alpha), \bar{I}(\alpha), \bar{F}(\alpha)\right) \quad (36)$$

$$\bar{T}(\alpha) = \begin{cases} T & 1 < \alpha \\ \overline{T_a} & 1 \geq \alpha \end{cases} \quad (37)$$

$$\overline{T_\alpha}(a,b) = \frac{1}{w*w}\sum_{k=a-w/2}^{a+w/2}\sum_{l=b-w/2}^{b+w/2} T(k,l) \quad (37(a))$$

$$\bar{F}(\alpha) = \begin{cases} F & 1 < \alpha \\ \overline{F_a} & 1 \geq \alpha \end{cases} \quad (38)$$

$$\overline{F_\alpha}(a,b) = \frac{1}{w*w}\sum_{k=a-w/2}^{a+w/2}\sum_{l=b-w/2}^{b+w/2} F(k,l) \quad (38(a))$$

$$\bar{I}(\alpha) = \begin{cases} T & 1 < \alpha \\ \overline{T_\alpha} & 1 \geq \alpha \end{cases} \quad (39)$$

$$\overline{I_\alpha}(a,b) = \frac{1}{w*w}\sum_{k=a-w/2}^{a+w/2}\sum_{l=b-w/2}^{b+w/2} I(k,l) \quad (39(a))$$

$$\overline{I_\alpha}(a,b) = \frac{\overline{\delta(a,b)} - \overline{\delta_{min}}}{\overline{\delta_{max}} - \overline{\delta_{min}}} \quad (39(b))$$

$$\overline{\delta(a,b)} = abs(\bar{T}(a,b) - \bar{\bar{T}}(a,b)) \quad (40)$$

$$\bar{\bar{T}}(a,b) = \frac{1}{w*w}\sum_{k=a-w/2}^{a+w/2}\sum_{l=b-w/2}^{b+w/2} \bar{T}(k,l) \quad (41)$$

Where, $\delta(a,b)$ is the absolute value of the variations between the mean intensity $(\bar{T}(a,b)$ and its mean value $\bar{\bar{T}}(a,b)$ after the α-mean operations. After the α-mean operation, the entropy of the indeterminate subset I is

The value of $I(a,b)$ is employed to measure the indeterminacy of element $P_{NS}(a,b)$. To make T and F correlated with I, the changes in T and F should influence the distribution of the elements and entropy of I. For a gray level image (H), the mean operation is provided in Eq. (35)

$$\omega'(a,b) = \begin{cases} 2\omega^2(a,b), & \omega(a,b) \leq 0.5 \\ 1 - 2\left(1 - \omega(a,b)\right)^2, & \omega(a,b) > 0.5 \end{cases} \quad (42)$$

increased and the distribution of the elements in I becomes more uniform.

- $\boldsymbol{\beta - enhancem}$**entoperations**

Infuzzy set, the intensification operation for the membership ω is termed in Eq. (42)

The $\beta - enhancement$ operations for P_{NS} i.e., P'_{NS} (β) is defined in Eq. (43-48).,

$$P'_{NS}(\beta) = P\left(T'(\beta), I'(\beta), F'(\beta)\right) \quad (43)$$

$$T'(\beta) = \begin{cases} T, & 1 < \beta \\ T'_\beta, & 1 \geq \beta \end{cases} \quad (44(a))$$

$$T'_\beta(a,b) = \begin{cases} 2T^2(a,b), & T(a,b) \leq 0.5 \\ 1 - 2\left(1 - T(a,b)\right)^2, & T(a,b) > 0.5 \end{cases} \quad (44(b))$$

$$F'(\beta) = \begin{cases} F & 1 < \beta \\ \overline{F_\beta} & 1 \geq \beta \end{cases} \quad (45)$$

$$F'_\beta(a,b) = \begin{cases} 2F^2(a,b), & F(a,b) \leq 0.5 \\ 1 - 2\left(1 - F(a,b)\right)^2, & F(a,b) > 0.5 \end{cases} \quad (45(b))$$

$$I'_{\beta}(a,b) = \frac{\delta'_T(a,b) - \delta'_{Tmin}}{\delta'_{Tmax} - \delta'_{Tmin}} \quad (46)$$

$$\delta'_T(a,b) = abs\,(T'(a,b) - \bar{T}'(a,b)) \quad (47)$$

$$\bar{T}'(a,b)) = \frac{1}{w*w}\sum_{k=a-w/2}^{a+w/2}\sum_{l=b-w/2}^{b+w/2} T'(k,l) \quad (48)$$

Where, $\delta'_T(a,b)$ is the absolute value of variations between intensity $T'(a,b)$ and its local mean value is represented as$\bar{T}'(a,b)$). After the $\beta-$ enhancement operation, the membership set T becomes more distinct which is suitable for CXR images segmentation tasks, as it removes the noise and retains detailed information.

3.5.2. Pre-processing using BTDRINI

Similarly, the two function like $\alpha - mean$ and $\beta - enhancements$ in NS domain is also used for the pre-processing tasks and reduces the indeterminacy of the BTDRINI set.

- ***α − mean* operations**

The value of $I(\,a_1, a_2, a_2, a_3, a_4\,;\, p_{B_iT}, q_{B_iT}, r_{B_iT}, s_{B_iT})$ is employed to measure the indeterminacy of element $\ddot{\mathcal{A}}_{B_iT}$. To make T and F correlated with I, the changes in T and F should influence the distribution of the elements and entropy of I. The $\alpha - mean$ operation for $\ddot{\mathcal{A}}_{B_iT}$ and $\overline{\ddot{\mathcal{A}}_{B_lT}}$is defined in Eq. (49).,

$$\overline{\ddot{\mathcal{A}}_{B_lT}}(\alpha) = P\left(\overline{a_1}, \overline{a_2}, \overline{a_3}, \overline{a_4}\,;\, \overline{p_{B_lT_\alpha}}, \overline{q_{B_lT_\alpha}}, \overline{r_{B_lT_\alpha}}, \overline{s_{B_lT_\alpha}}\right) \quad (49)$$

$\overline{\ddot{\mathcal{A}}_{B_lT}}(\alpha)$interpret the BTDRINI memberships to $\overline{T_\alpha{}^+}(x)$, $\overline{T_\alpha{}^-}(x)$, $\overline{I_{T_\alpha}{}^+}(x)$, $\overline{I_{T_\alpha}{}^-}(x)$, $\overline{I_{F_\alpha}{}^+}(x)$, $\overline{I_{F_\alpha}{}^-}(x)$, $\overline{F_\alpha{}^+}(x)$ and $\overline{F_\alpha{}^-}(x)$ which is represented in the table 4 following Eqs. (50(a-h)).

Table 4 $\alpha - mean$ operations in BTDRINSS for pre-processing

Positive Degree of Truth-Membership	**Negative Degree of Truth-Membership**
$\overline{T_\alpha{}^+}(x) = \begin{cases} \overline{p_{B_lT_\alpha}}\frac{x-\overline{a_1}}{\overline{a_2}-\overline{a_1}}\overline{a_1} \le x < \overline{a_2} \\ \overline{p_{B_lT_\alpha}}\overline{a_2} \le x \le \overline{a_3} \\ \overline{p_{B_lT_\alpha}}\frac{\overline{a_4}-x}{\overline{a_4}-\overline{a_3}}\overline{a_3} < x \le \overline{a_4} \\ 0 \quad otherwise \end{cases}$ (50(a))	$\overline{T_\alpha{}^-}(x) = \begin{cases} \overline{p_{B_lT_\alpha}}\frac{x-\overline{a_1}}{\overline{a_2}-\overline{a_1}}\overline{a_1} \le x < \overline{a_2} \\ -\overline{p_{B_lT_\alpha}}\overline{a_2} \le x \le \overline{a_3} \\ \overline{p_{B_lT_\alpha}}\frac{\overline{a_4}-x}{\overline{a_4}-\overline{a_3}}\overline{a_3} < x \le \overline{a_4} \\ 0 \quad otherwise \end{cases}$ (50(b))
Positive degree of Indeterminate toward Truth Membership	**Negative degree of indeterminate towards Truth membership**
$\overline{I_{T_\alpha}{}^+}(x) = \begin{cases} \overline{q_{B_lT_\alpha}}\frac{x-\overline{a_1}}{\overline{a_2}-\overline{a_1}}\overline{a_1} \le x < \overline{a_2} \\ \overline{q_{B_lT_\alpha}}\overline{a_2} \le x \le \overline{a_3} \\ \overline{q_{B_lT_\alpha}}\frac{\overline{a_4}-x}{\overline{a_4}-\overline{a_3}}\overline{a_3} < x \le \overline{a_4} \\ 0 \quad otherwise \end{cases}$ (50(c))	$\overline{I_{T_\alpha}{}^-}(x) = \begin{cases} \overline{q_{B_lT_\alpha}}\frac{x-\overline{a_1}}{\overline{a_2}-\overline{a_1}}\overline{a_1} \le x < \overline{a_2} \\ -\overline{q_{B_lT_\alpha}}\overline{a_2} \le x \le \overline{a_3} \\ \overline{q_{B_lT_\alpha}}\frac{\overline{a_4}-x}{\overline{a_4}-\overline{a_3}}\overline{a_3} < x \le \overline{a_4} \\ 0 \quad otherwise \end{cases}$ (50(d))
Positive Degree of Indeterminate Toward Falsity Membership	**Negative Degree of Indeterminate toward Falsity Membership**
$\overline{I_{F_\alpha}{}^+}(x) = \begin{cases} \frac{\overline{a_2}-x+\overline{r_{B_lT_\alpha}}(x-\overline{a_1})}{\overline{a_2}-\overline{a_1}}\overline{a_1} \le x < \overline{a_2} \\ \overline{r_{B_lT_\alpha}}\overline{a_2} \le x \le \overline{a_3} \\ \frac{x-\overline{a_3}+\overline{r_{B_lT_\alpha}}(\overline{a_4}-x)}{\overline{a_4}-\overline{a_3}}\overline{a_3} \le x \le \overline{a_4} \\ 1 \quad otherwise \end{cases}$ (50(e))	$\overline{I_{F_\alpha}{}^-}(x) = \begin{cases} \frac{x-\overline{a_2}+\overline{r_{B_lT_\alpha}}(\overline{a_1}-x)}{\overline{a_2}-\overline{a_1}}\overline{a_1} \le x < \overline{a_2} \\ -\overline{r_{B_lT_\alpha}}\overline{a_2} \le x \le \overline{a_3} \\ \frac{\overline{a_3}-x+\overline{r_{B_lT_\alpha}}(x-\overline{a_4})}{\overline{a_4}-\overline{a_3}}\overline{a_3} \le x \le \overline{a_4} \\ -1 \quad otherwise \end{cases}$ (50(f))
Positive degree of Falsity membership	**Negative degree of Falsity membership**
$\overline{F_\alpha{}^+}(x) = \begin{cases} \frac{\overline{a_2}-x+\overline{s_{B_lT_\alpha}}(x-\overline{a_1})}{\overline{a_2}-\overline{a_1}}\overline{a_1} \le x < \overline{a_2} \\ \overline{s_{B_lT_\alpha}}\overline{a_2} \le x \le \overline{a_3} \\ \frac{x-\overline{a_3}+\overline{s_{B_lT_\alpha}}(\overline{a_4}-x)}{\overline{a_4}-\overline{a_3}}\overline{a_3} \le x \le \overline{a_4} \\ 1 \quad otherwise \end{cases}$ (50(g))	$\overline{F_\alpha{}^-}(x) = \begin{cases} \frac{x-\overline{a_2}+\overline{r_{B_lT_\alpha}}(\overline{a_1}-x)}{\overline{a_2}-\overline{a_1}}\overline{a_1} \le x < \overline{a_2} \\ -\overline{r_{B_lT_\alpha}}\overline{a_2} \le x \le \overline{a_3} \\ \frac{\overline{a_3}-x+\overline{r_{B_lT_\alpha}}(x-\overline{a_4})}{\overline{a_4}-\overline{a_3}}\overline{a_3} \le x \le \overline{a_4} \\ -1 \quad otherwise \end{cases}$ (50(h))

Finally,

$$\delta\left(\overline{a_1},\overline{a_2},\overline{a_3},\overline{a_4}\,;\,\overline{p_{B_iT_\alpha}}\,,\overline{q_{B_iT_\alpha}},\overline{r_{B_iT_\alpha}},\overline{s_{B_iT_\alpha}}\right)=(a_1,a_2,a_2,a_3,a_4\,;\,p_{B_iT}\,,q_{B_iT},r_{B_iT},s_{B_iT})$$

$$(((\overline{T_\alpha}^{+}(x),\overline{T_\alpha}^{-}(\alpha)),\overline{I_{T_\alpha}}^{+}(x),\overline{I_{T_\alpha}}^{-}(x),\overline{I_{F_\alpha}}^{+}(x),\overline{I_{F_\alpha}}^{-}(x),\overline{F_\alpha}^{+}(\alpha)\overline{F_\alpha}^{-}(x))-\overline{\overline{T_\alpha}^{+}}(x),\overline{\overline{T_\alpha}^{-}}(x)),\overline{\overline{I_{T_\alpha}}^{+}}(x),\overline{\overline{I_{T_\alpha}}^{-}}(x),$$
$$\overline{\overline{I_{F_\alpha}}^{+}}(x),\overline{\overline{I_{F_\alpha}}^{-}}(x),\overline{\overline{F_\alpha}^{+}}(x),\overline{\overline{F_\alpha}^{-}}(x)\,)\ (51)$$

Where, $\delta\left(\overline{a_1},\overline{a_2},\overline{a_3},\overline{a_4}\,;\,\overline{p_{B_iT}}\,,\overline{q_{B_iT}},\overline{r_{B_iT}},\overline{s_{B_iT}}\right)$is the absolute value of the variations between the mean intensity of positive and negative degree of BTDRINSS and its mean value $\overline{\overline{T_\alpha}^{+}}(x),\overline{\overline{T_\alpha}^{-}}(x)),\overline{\overline{I_{T_\alpha}}^{+}}(x),$ $\overline{\overline{I_{T_\alpha}}^{-}}(x),\overline{\overline{I_{F_\alpha}}^{+}}(x),\overline{\overline{I_{F_\alpha}}^{-}}(x),\overline{\overline{F_\alpha}^{+}}(x),\overline{\overline{F_\alpha}^{-}}(x)\,)$. After the α-mean operation, the entropy of the indeterminate subset BTDRINI is increased and the distribution of the elements in I becomes more uniform.

- $\boldsymbol{\beta-enhancement}$ **operations**

In fuzzy set, the intensification operation for the BTDRINI membership ω is termed in Eq. (52)

$$\omega'\left(a_1,a_2,a_2,a_3,a_4\,;\,p_{B_iT}\,,q_{B_iT},r_{B_iT},s_{B_iT}\right)$$
$$=\begin{cases}2\omega^2\left(a_1,a_2,a_2,a_3,a_4\,;\,p_{B_iT}\,,q_{B_iT},r_{B_iT},s_{B_iT}\right), & \omega\left(a_1,a_2,a_2,a_3,a_4\,;\,p_{B_iT}\,,q_{B_iT},r_{B_iT},s_{B_iT}\right)\le 0.5\\ 1-2\left(1-\omega\left(a_1,a_2,a_2,a_3,a_4\,;\,p_{B_iT}\,,q_{B_iT},r_{B_iT},s_{B_iT}\right)\right)^2, & \omega\left(a_1,a_2,a_2,a_3,a_4\,;\,p_{B_iT}\,,q_{B_iT},r_{B_iT},s_{B_iT}\right)>0.5\end{cases}\quad(52)$$

The $\beta-enhancemnet$ operations for $\ddot{\mathcal{A}}_{B_iT}$i.e., $\ddot{\mathcal{A}}_{B_iT}{}'(\beta)$ is defined in Eq. (54(a-h))

$$\ddot{\mathcal{A}}_{B_iT}{}'(\beta)=P\left(a_1,a_2,a_3,a_4\,;\,p_{B_iT_\beta}\,,q_{B_iT_\beta},r_{B_iT_\beta},s_{B_iT_\beta}\right)(53)$$

$\ddot{\mathcal{A}}_{B_iT}(\beta)$interpret the BTDRINI memberships to ${T_\beta}^{+}(x),{T_\beta}^{-}(x),{I_{T_\beta}}^{+}(x),{I_{T_\beta}}^{-}(x),{I_{F_\beta}}^{+}(x),{I_{F_\beta}}^{-}(x),{F_\beta}^{+}(x)$ and ${F_\beta}^{-}(x)$

Table 5. $\boldsymbol{\beta-enhancement}$ Operations in BTDRINSS for Pre-processing

Positive Degree of Truth-Membership	**Negative Degree of Truth-Membership**
$T_\beta{}^{+}(x)=\begin{cases}p_{B_iT_\beta}\frac{x-a_1}{a_2-a_1}a_1\ \le x<a_2\\ p_{B_iT_\beta}a_2\ \le x\le a_3\\ p_{B_iT_\beta}\frac{a_4-x}{a_4-a_3}a_3<x\ \le a_4\\ 0\quad otherwise\end{cases}$ (54(a))	$T_\beta{}^{-}(x)=\begin{cases}p_{B_iT_\beta}\frac{a_1-x}{a_2-a_1}a_1\ \le x<a_2\\ -p_{B_iT_\beta}a_2\ \le x\le a_3\\ p_{B_iT_\beta}\frac{x-a_4}{a_4-a_3}a_3<x\ \le a_4\\ 0\quad otherwise\end{cases}$ (54(b))
Positive degree of Indeterminate toward Truth Membership	**Negative degree of indeterminate towards truth membership**
${I_{T_\beta}}^{+}(x)=\begin{cases}q_{B_iT_\beta}\frac{x-a_1}{a_2-a_1}a_1\ \le x<a_2\\ q_{B_iT_\beta}a_2\ \le x\le a_3\\ q_{B_iT_\beta}\frac{a_4-x}{a_4-a_3}a_3<x\ \le a_4\\ 0\quad otherwise\end{cases}$ (54(c))	${I_{T_\beta}}^{-}(x)=\begin{cases}q_{B_iT_\beta}\frac{a_1-x}{a_2-a_1}a_1\ \le x<a_2\\ -q_{B_iT_\beta}a_2\ \le x\le a_3\\ q_{B_iT_\beta}\frac{x-a_4}{a_4-a_3}a_3<x\ \le a_4\\ 0\quad otherwise\end{cases}$ (54(d))
Positive Degree Of Indeterminate Toward Falsity Membership	**Negative Degree Of Indeterminate toward Falsity Membership**
${I_{F_\beta}}^{+}(x)=\begin{cases}\frac{a_2-x+r_{B_iT_\beta}(x-a_1)}{a_2-a_1}a_1\ \le x<a_2\\ r_{B_iT_\beta}a_2\ \le x\le a_3\\ \frac{x-a_3+r_{B_iT_\beta}(a_4-x)}{a_4-a_3}a_3<x\ \le a_4\\ 1\quad otherwise\end{cases}$ (54(e))	${I_{F_\beta}}^{-}(x)=\begin{cases}\frac{x-a_2+r_{B_iT_\beta}(a_1-x)}{a_2-a_1}a_1\ \le x<a_2\\ -r_{B_iT_\beta}a_2\ \le x\le a_3\\ \frac{a_3-x+r_{B_iT_\beta}(x-a_4)}{a_4-a_3}a_3<x\ \le a_4\\ -1\quad otherwise\end{cases}$ (54(f))
Positive degree of Falsity membership	**Negative degree of Falsity membership**
$F_\beta{}^{+}(x)=\begin{cases}\frac{a_2-x+s_{B_iT_\beta}(x-a_1)}{a_2-a_1}a_1\ \le x<a_2\\ s_{B_iT_\beta}a_2\ \le x\le a_3\\ \frac{x-a_3+s_{B_iT_\beta}(a_4-x)}{a_4-a_3}a_3<x\ \le a_4\\ 1\quad otherwise\end{cases}$ (54(g))	$F^{-}(x)=\begin{cases}\frac{x-a_2+s_{B_iT_\beta}(a_1-x)}{a_2-a_1}a_1\ \le x<a_2\\ -s_{B_iT_\beta}a_2\ \le x\le a_3\\ \frac{a_3-x+s_{B_iT_\beta}(x-a_4)}{a_4-a_3}a_3<x\ \le a_4\\ -1\quad otherwise\end{cases}$ (54(h))

Finally,

$$\delta\left(a_1, a_2, a_2, a_3, a_4\ ;\ p_{B_iT_\beta}, q_{B_iT_\beta}, r_{B_iT_\beta}, s_{B_iT_\beta}\right) = (a_1, a_2, a_2, a_3, a_4\ ;\ p_{B_iT_\beta}, q_{B_iT_\beta}, r_{B_iT_\beta}, s_{B_iT_\beta})$$
$$(((\overline{T_\beta}^{+}(x), \overline{T_\beta}^{-}(\alpha)), \overline{I_{T_\beta}}^{+}(x), \overline{I_{T_\beta}}^{-}(x), \overline{I_{F_\beta}}^{+}(x), \overline{I_{F_\beta}}^{-}(x), \overline{F_\beta}^{+}(x)\overline{F_\beta}^{-}(x)) - \overline{\overline{T_\beta}^{+}}(x), \overline{\overline{T_\beta}^{-}}(x)), \overline{\overline{I_{T_\beta}}^{+}}(x), \overline{\overline{I_{T_\beta}}^{-}}(x),$$
$$\overline{\overline{I_{F_\beta}}^{+}}(x), \overline{\overline{I_{F_\beta}}^{-}}(x), \overline{\overline{F_\beta}^{+}}(x), \overline{\overline{F_\beta}^{-}}(x)\ ) \qquad (55)$$

Where, $\delta(\overline{a_1}, \overline{a_2}, \overline{a_3}, \overline{a_4}\ ;\ \overline{p_{B_iT}}\ , \overline{q_{B_iT}}, \overline{r_{B_iT}}, \overline{s_{B_iT}})$is the absolute value of the variations between the mean intensity of positive and negative degree of BTDRINSS and its mean value $\overline{\overline{T_\beta}^{+}}(x)$, $\overline{\overline{T_\beta}^{-}}(x))$, $\overline{\overline{I_{T_\beta}}^{+}}(x)$, $\overline{\overline{I_{T_\beta}}^{-}}(x), \overline{\overline{I_{F_\beta}}^{+}}(x), \overline{\overline{I_{F_\beta}}^{-}}(x), \overline{\overline{T_\beta}^{+}}(x), \overline{\overline{T_\beta}^{-}}(x)\ )$.

After the $\beta-$ enhancement operation, the membership set of BTDRINI in which Icomes more distinct which is suitable for CXR images segmentation tasks, as it removes the noise and retains detailed information.

3.5.3 Pre-processing using GBTDRINI

As like NS domain, the GBTDRINI also adopts for two operations like $\alpha - mean$ and $\beta - enhancemnts$ in GBTDRINSS domain is used for the pre-processing tasks and reduces the indeterminacy of the GBTDRINI set.

- **$\alpha -$ *mean* operations**

The value of $I(\bar{\bar{\mathcal{A}}}_t, \bar{\bar{\mathcal{A}}}_{it}, \bar{\bar{\mathcal{A}}}_{if}, \bar{\bar{\mathcal{A}}}_f$ and $\bar{\bar{\mathcal{B}}}_t, \bar{\bar{\mathcal{B}}}_{it}, \bar{\bar{\mathcal{B}}}_{if}, \bar{\bar{\mathcal{B}}}_f)$ is employed to measure the indeterminacy of element $\bar{\bar{\mathcal{A}}}_{GN}, \bar{\bar{\mathcal{B}}}_{GN}$. The α-mean operations for $\bar{\bar{\mathcal{A}}}_{GN}$and $\overline{\bar{\bar{\mathcal{A}}}_{GN}}$ is defined in () as like α-mean operations for $\bar{\bar{\mathcal{B}}}_{GN}$and $\overline{\bar{\bar{\mathcal{B}}}_{GN}}$ is illustrated in Eq. (56) and (57)

$$\overline{\bar{\bar{\mathcal{A}}}_{GN}}(\alpha) = P(\overline{\bar{\bar{\mathcal{A}}}_t}(\alpha), \overline{\bar{\bar{\mathcal{A}}}_{it}}(\alpha), \overline{\bar{\bar{\mathcal{A}}}_{if}}(\alpha), \overline{\bar{\bar{\mathcal{A}}}_f}(\alpha)) \qquad (56)$$

$$\overline{\bar{\bar{\mathcal{B}}}_{GN}}(\alpha) = P(\overline{\bar{\bar{\mathcal{B}}}_t}(\alpha), \overline{\bar{\bar{\mathcal{B}}}_{it}}(\alpha), \overline{\bar{\bar{\mathcal{B}}}_{if}}(\alpha), \overline{\bar{\bar{\mathcal{B}}}_f}(\alpha)) \qquad (57)$$

$\overline{\bar{\bar{\mathcal{A}}}_{GN}}(\alpha)$and $\overline{\bar{\bar{\mathcal{B}}}_{GN}}(\alpha)$ interprets the GBTDRINI memberships value which is represented in the following Eqs. (58 (a-h)).

$$\overline{\bar{\bar{\mathcal{A}}}_t}(\alpha) = \begin{cases} (\bar{\mu}_{\bar{\bar{\mathcal{A}}}_t(\alpha)} - \sigma_{\bar{\bar{\mathcal{A}}}_t(\alpha)}\sqrt{-2\log\alpha}\ , \bar{\mu}_{\bar{\bar{\mathcal{A}}}_t(\alpha)} + \sigma_{\overline{\bar{\bar{\mathcal{A}}}_t(\alpha)}}\sqrt{-2\log\alpha}) & 1 < \alpha \\ (\bar{\mu}_{\bar{\bar{\mathcal{A}}}_t(\alpha)} - \sigma_{\bar{\bar{\mathcal{A}}}_t(\alpha)}\sqrt{-2\log\alpha}\ , \bar{\mu}_{\bar{\bar{\mathcal{A}}}_t(\alpha)} + \sigma_{\bar{\bar{\mathcal{A}}}_{t(\alpha)\,t}}\sqrt{-2\log\alpha}) & 1 \geq \alpha \end{cases} \quad 58(a)$$

$$\overline{\bar{\bar{\mathcal{B}}}_t}(\alpha) = \begin{cases} (\bar{\mu}_{\bar{\bar{\mathcal{B}}}_t(\alpha)} - \sigma_{\bar{\bar{\mathcal{B}}}_t(\alpha)}\sqrt{-2\log\alpha}\ , \bar{\mu}_{\bar{\bar{\mathcal{B}}}_t(\alpha)} + \sigma_{\overline{\bar{\bar{\mathcal{B}}}_t(\alpha)}}\sqrt{-2\log\alpha}) & 1 < \alpha \\ (\bar{\mu}_{\bar{\bar{\mathcal{B}}}_t(\alpha)} - \sigma_{\bar{\bar{\mathcal{B}}}_t}\sqrt{-2\log\alpha}\ , \bar{\mu}_{\bar{\bar{\mathcal{B}}}_t(\alpha)} + \sigma_{\overline{\bar{\bar{\mathcal{B}}}_t(\alpha)}}\sqrt{-2\log\alpha}) & 1 \geq \alpha \end{cases} \quad 58(b)$$

$$\overline{\bar{\bar{\mathcal{A}}}_{it}}(\alpha) = \begin{cases} (\bar{\mu}_{\bar{\bar{\mathcal{A}}}_{it}(\alpha)} - \sigma_{\bar{\bar{\mathcal{A}}}_{it}}\sqrt{-2\log\alpha}\ , \bar{\mu}_{\bar{\bar{\mathcal{A}}}_{it}(\alpha)} + \sigma_{\bar{\bar{\mathcal{A}}}_{it}(\alpha)}\sqrt{-2\log\alpha}) & 1 < \alpha \\ (\bar{\mu}_{\bar{\bar{\mathcal{A}}}_{it}(\alpha)} - \sigma_{\bar{\bar{\mathcal{A}}}_{it}(\alpha)}\sqrt{-2\log\alpha}\ , \bar{\mu}_{\bar{\bar{\mathcal{A}}}_{it}(\alpha)} + \sigma_{\bar{\bar{\mathcal{A}}}_{it}(\alpha)}\sqrt{-2\log\alpha}) & 1 \geq \alpha \end{cases} \quad 58(c)$$

$$\overline{\bar{\bar{\mathcal{B}}}_{it}}(\alpha) = \begin{cases} (\bar{\mu}_{\bar{\bar{\mathcal{B}}}_{it}(\alpha)} - \sigma_{(\bar{\bar{\mathcal{B}}}_{it}(\alpha))}\sqrt{-2\log\alpha}\ , \bar{\mu}_{\bar{\bar{\mathcal{B}}}_{it}(\alpha)} + \sigma_{\bar{\bar{\mathcal{B}}}_{it}(\alpha)}\sqrt{-2\log\alpha}) & 1 < \alpha \\ (\bar{\mu}_{\bar{\bar{\mathcal{B}}}_{it}(\alpha)} - \sigma_{\bar{\bar{\mathcal{B}}}_{it}(\alpha)}\sqrt{-2\log\alpha}\ , \bar{\mu}_{\bar{\bar{\mathcal{B}}}_{it}(\alpha)} + \sigma_{\bar{\bar{\mathcal{B}}}_{it}(\alpha)}\sqrt{-2\log\alpha}) & 1 \geq \alpha \end{cases} \quad 58(d)$$

$$\overline{\bar{\bar{\mathcal{A}}}_{if}}(\alpha) = \begin{cases} (\bar{\mu}_{\bar{\bar{\mathcal{A}}}_{if}(\alpha)} - \sigma_{\bar{\bar{\mathcal{A}}}_{if}(\alpha)}\sqrt{-2\log\alpha}\ , \bar{\mu}_{\bar{\bar{\mathcal{A}}}_{if}(\alpha)} + \sigma_{\bar{\bar{\mathcal{A}}}_{if}(\alpha)}\sqrt{-2\log\alpha}) & 1 < \alpha \\ (\bar{\mu}_{\bar{\bar{\mathcal{A}}}_{if}(\alpha)} - \sigma_{\bar{\bar{\mathcal{A}}}_{if}(\alpha)}\sqrt{-2\log\alpha}\ , \bar{\mu}_{\bar{\bar{\mathcal{A}}}_{if}(\alpha)} + \sigma_{\bar{\bar{\mathcal{A}}}_{if}(\alpha)}\sqrt{-2\log\alpha}) & 1 \geq \alpha \end{cases} \quad 58(e)$$

$$\overline{\bar{\bar{\mathcal{B}}}_{if}}(\alpha) = \begin{cases} (\bar{\mu}_{\bar{\bar{\mathcal{B}}}_{if}(\alpha)} - \sigma_{\bar{\bar{\mathcal{B}}}_{if}(\alpha)}\sqrt{-2\log\alpha}\ , \bar{\mu}_{\bar{\bar{\mathcal{B}}}_{if}(\alpha)} + \sigma_{\bar{\bar{\mathcal{B}}}_{if}(\alpha)}\sqrt{-2\log\alpha}) & 1 < \alpha \\ (\bar{\mu}_{\bar{\bar{\mathcal{B}}}_{if}(\alpha)} - \sigma_{\bar{\bar{\mathcal{B}}}_{if}(\alpha)}\sqrt{-2\log\alpha}\ , \bar{\mu}_{\bar{\bar{\mathcal{B}}}_{if}(\alpha)} + \sigma_{\bar{\bar{\mathcal{B}}}_{if}(\alpha)}\sqrt{-2\log\alpha}) & 1 \geq \alpha \end{cases} \quad 58(f)$$

$$\overline{\bar{\bar{\mathcal{A}}}_f}(\alpha) = \begin{cases} (\bar{\mu}_{\bar{\bar{\mathcal{A}}}_f(\alpha)} - \sigma_{\bar{\bar{\mathcal{A}}}_f(\alpha)}\sqrt{-2\log\alpha}\ , \bar{\mu}_{\bar{\bar{\mathcal{A}}}_f(\alpha)} + \sigma_{\bar{\bar{\mathcal{A}}}_f(\alpha)}\sqrt{-2\log\alpha}) & 1 < \alpha \\ (\bar{\mu}_{\bar{\bar{\mathcal{A}}}_f(\alpha)} - \sigma_{\bar{\bar{\mathcal{A}}}_f(\alpha)}\sqrt{-2\log\alpha}\ , \bar{\mu}_{\bar{\bar{\mathcal{A}}}_f(\alpha)} + \sigma^{-}_{\bar{\bar{\mathcal{A}}}_f(\alpha)}\sqrt{-2\log\alpha}) & 1 \geq \alpha \end{cases} \quad 58(g)$$

$$\overline{\bar{\bar{\mathcal{B}}}_f}(\alpha) = \begin{cases} (\bar{\mu}_{\bar{\bar{\mathcal{B}}}_f(\alpha)} - \sigma_{\bar{\bar{\mathcal{B}}}_f(\alpha)}\sqrt{-2\log\alpha}\ , \bar{\mu}_{\bar{\bar{\mathcal{B}}}_f(\alpha)} + \sigma_{\bar{\bar{\mathcal{B}}}_f(\alpha)}\sqrt{-2\log\alpha}) & 1 < \alpha \\ (\bar{\mu}_{\bar{\bar{\mathcal{B}}}_f(\alpha)} - \sigma_{\bar{\bar{\mathcal{B}}}_f(\alpha)}\sqrt{-2\log\alpha}\ , \sigma_{\bar{\bar{\mathcal{B}}}_f(\alpha)} + \sigma_{\bar{\bar{\mathcal{B}}}_f(\alpha)}\sqrt{-2\log\alpha}) & 1 \geq \alpha \end{cases} \quad 58(h)$$

Finally,

$$\delta\left(\overline{\bar{\bar{\mathcal{A}}}_{GN}}(\alpha)\right) = (\overline{\bar{\bar{\mathcal{A}}}_{GN}}(\alpha)\,.\,(\bar{\bar{\mathcal{A}}}_{t(\alpha)}, \bar{\bar{\mathcal{A}}}_{it()}, \bar{\bar{\mathcal{A}}}_{if(\alpha)}, \bar{\bar{\mathcal{A}}}_{f(\alpha)})) \quad (59)$$

$$\delta\left(\overline{\bar{\bar{\mathcal{B}}}_{GN}}(\alpha)\right) = (\overline{\bar{\bar{\mathcal{B}}}_{GN}}(\alpha)\,.\,(\bar{\bar{\mathcal{B}}}_{t(\alpha)}, \bar{\bar{\mathcal{B}}}_{it(\alpha)}, \bar{\bar{\mathcal{B}}}_{if(\alpha)}, \bar{\bar{\mathcal{B}}}_{f(\alpha)})) \quad (60)$$

Where, $\delta\left(\overline{\bar{\mathcal{A}}_t}(\alpha),\overline{\bar{\mathcal{A}}_{it}}(\alpha),\overline{\bar{\mathcal{A}}_{if}}(\alpha),\overline{\bar{\mathcal{A}}_f}(\alpha);\overline{\bar{B}_t}(\alpha),\overline{\bar{B}_{it}}(\alpha),\overline{\bar{B}_{if}}(\alpha),\overline{\bar{B}_f}(\alpha)\right)$ is the absolute value of the variations between the mean intensity $\bar{\bar{\mathcal{A}}}_{GN}(\alpha)$and $\bar{\bar{B}}_{GN}(\alpha)$its meanvalue $\overline{\bar{\bar{\mathcal{A}}}_t}(\alpha)$and $\overline{\bar{\bar{B}}_t}(\alpha)$. After the α-mean operation, the entropy of the indeterminate subset GBTDRINI is increased and the distribution of the elements in I becomes more uniform.

- $\boldsymbol{\beta - mean}$ **operations**

In fuzzy set, the intensification operation for the GBTDRINI membership ω is termed in Eq. (61) and (62)

$$\omega'\left(\overline{\bar{\bar{\mathcal{A}}}_{GN}}\right)=\begin{cases}2\omega^2(\bar{\bar{\mathcal{A}}}_t,\bar{\bar{\mathcal{A}}}_{it},\bar{\bar{\mathcal{A}}}_{if},\bar{\bar{\mathcal{A}}}_f), & \omega(\overline{\bar{\bar{\mathcal{A}}}_t},\bar{\bar{\mathcal{A}}}_{it},\bar{\bar{\mathcal{A}}}_{if},\bar{\bar{\mathcal{A}}}_f)\le 0.5\\ 1-2(\ \bar{\bar{\mathcal{A}}}_t,\bar{\bar{\mathcal{A}}}_{it},\bar{\bar{\mathcal{A}}}_{if},\bar{\bar{\mathcal{A}}}_f)^2, & \omega(\bar{\bar{\mathcal{A}}}_t,\bar{\bar{\mathcal{A}}}_{it},\bar{\bar{\mathcal{A}}}_{if},\bar{\bar{\mathcal{A}}}_f)>0.5\end{cases} \quad (61)$$

$$\omega'\left(\overline{\bar{\bar{B}}_{GN}}\right)=\begin{cases}2\omega^2\ (\bar{\bar{B}}_t,\bar{\bar{B}}_{it},\bar{\bar{B}}_{if},\bar{\bar{B}}_f), & \omega\ (\bar{\bar{B}}_t,\bar{\bar{B}}_{it},\bar{\bar{B}}_{if},\bar{\bar{B}}_f))\le 0.5\\ 1-2\ (\bar{\bar{B}}_t,\bar{\bar{B}}_{it},\bar{\bar{B}}_{if},\bar{\bar{B}}_f)^2, & \omega(\bar{\bar{B}}_t,\bar{\bar{B}}_{it},\bar{\bar{B}}_{if},\bar{\bar{B}}_f))>0.5\end{cases} \quad (62)$$

The $\beta - enhancement$ operations for $\overline{\bar{\bar{\mathcal{A}}}_{GN}}$ and $\overline{\bar{B}_{GN}}$, i.e., $\overline{\bar{\bar{\mathcal{A}}}_{GN}}(\beta)$ and $\overline{\bar{\bar{B}}_{GN}}(\beta)$is defined in Eq. (63) and (64)

$$\overline{\bar{\bar{\mathcal{A}}}_{GN}}(\beta)=P(\overline{\bar{\bar{\mathcal{A}}}_t}(\beta),\overline{\bar{\bar{\mathcal{A}}}_{it}}(\beta),\overline{\bar{\bar{\mathcal{A}}}_{if}}(\beta),\overline{\bar{\bar{\mathcal{A}}}_f}(\beta)); \quad (63)$$

$$\overline{\bar{\bar{B}}_{GN}}(\beta)=P(\overline{\bar{\bar{B}}_t}(\beta),\overline{\bar{\bar{B}}_{it}}(\beta),\overline{\bar{\bar{B}}_{if}}(\beta),\overline{\bar{\bar{B}}_f}(\beta)) \quad (64)$$

$\overline{\bar{\bar{\mathcal{A}}}_{GN}}(\beta)$ and $\overline{\bar{\bar{B}}_{GN}}(\beta)$ interpret the GBTDRINI memberships which is represented in the following Eq. (65(a-h))

$$\overline{\bar{\bar{\mathcal{A}}}_t}(\beta)=\begin{cases}(\bar{\mu}_{\bar{\bar{\mathcal{A}}}_t(\beta)}-\sigma_{\bar{\bar{\mathcal{A}}}_t(\beta)}\sqrt{-2\log\alpha}\ ,\bar{\mu}_{\bar{\bar{\mathcal{A}}}_t(\beta)}+\sigma_{\overline{\bar{\bar{\mathcal{A}}}_t}(\beta)}\sqrt{-2\log\alpha}) & 1<\beta\\ (\bar{\mu}_{\bar{\bar{\mathcal{A}}}_t(\beta)}-\sigma_{\bar{\bar{\mathcal{A}}}_t(\beta)}\sqrt{-2\log\alpha}\ ,\bar{\mu}_{\bar{\bar{\mathcal{A}}}_t(\beta)}+\sigma_{\bar{\bar{\mathcal{A}}}_t(\beta)}\sqrt{-2\log\alpha}) & 1\ge\beta\end{cases} \quad (65(a))$$

$$\overline{\bar{\bar{B}}_t}(\beta)=\begin{cases}(\bar{\mu}_{\bar{\bar{B}}_t(\beta)}-\sigma_{\bar{\bar{B}}_t(\beta)}\sqrt{-2\log\alpha}\ ,\bar{\mu}_{\bar{\bar{B}}_t(\beta)}+\sigma_{\overline{\bar{\bar{B}}_t}(\beta)}\sqrt{-2\log\alpha}) & 1<\beta\\ (\bar{\mu}_{\bar{\bar{B}}_t(\beta)}-\sigma_{\bar{\bar{B}}_t(\beta)}\sqrt{-2\log\alpha}\ ,\bar{\mu}_{\bar{\bar{B}}_t(\beta)}+\sigma_{\overline{\bar{\bar{B}}_t}(\beta)}\sqrt{-2\log\alpha}) & 1\ge\beta\end{cases} \quad (65(b))$$

$$\overline{\bar{\bar{\mathcal{A}}}_{it}}(\beta)=\begin{cases}(\bar{\mu}_{\bar{\bar{\mathcal{A}}}_{it}(\beta)}-\sigma_{\bar{\bar{\mathcal{A}}}_{it}(\beta)}\sqrt{-2\log\alpha}\ ,\bar{\mu}_{\bar{\bar{\mathcal{A}}}_{it}(\beta)}+\sigma_{\bar{\bar{\mathcal{A}}}_{it}(\beta)}\sqrt{-2\log\alpha}) & 1<\beta\\ (\bar{\mu}_{\bar{\bar{\mathcal{A}}}_{it}(\beta)}-\sigma_{\bar{\bar{\mathcal{A}}}_{it}(\beta)}\sqrt{-2\log\alpha}\ ,\bar{\mu}_{\bar{\bar{\mathcal{A}}}_{it}(\beta)}+\sigma_{\bar{\bar{\mathcal{A}}}_{it}(\beta)}\sqrt{-2\log\alpha}) & 1\ge\beta\end{cases} \quad (65(c))$$

$$\overline{\bar{\bar{B}}_{it}}(\beta)=\begin{cases}(\bar{\mu}_{\bar{\bar{B}}_{it}(\beta)}-\sigma_{(\bar{\bar{B}}_{it}(\beta)}\sqrt{-2\log\alpha}\ ,\bar{\mu}_{\bar{\bar{B}}_{it}(\beta)}+\sigma_{\bar{\bar{B}}_{it}(\beta)}\sqrt{-2\log\alpha}) & 1<\beta\\ (\bar{\mu}_{\bar{\bar{B}}_{it}(\beta)}-\sigma_{\bar{\bar{B}}_{it}(\beta)}\sqrt{-2\log\alpha}\ ,\bar{\mu}_{\bar{\bar{B}}_{it}(\beta)}+\sigma_{\bar{\bar{B}}_{it}(\beta)}\sqrt{-2\log\alpha}) & 1\ge\beta\end{cases} \quad (65(d))$$

$$\overline{\bar{\bar{\mathcal{A}}}_{if}}(\beta)=\begin{cases}(\bar{\mu}_{\bar{\bar{\mathcal{A}}}_{if}(\beta)}-\sigma_{\bar{\bar{\mathcal{A}}}_{if}(\beta)}\sqrt{-2\log\alpha}\ ,\bar{\mu}_{\bar{\bar{\mathcal{A}}}_{if}(\beta)}+\sigma_{\bar{\bar{\mathcal{A}}}_{if}(\beta)}\sqrt{-2\log\alpha}) & 1<\beta\\ (\bar{\mu}_{\bar{\bar{\mathcal{A}}}_{if}(\beta)}-\sigma_{\bar{\bar{\mathcal{A}}}_{if}(\beta)}\sqrt{-2\log\alpha}\ ,\bar{\mu}_{\bar{\bar{\mathcal{A}}}_{if}(\beta)}+\sigma_{\bar{\bar{\mathcal{A}}}_{if}(\beta)}\sqrt{-2\log\alpha}) & 1\ge\beta\end{cases} \quad (65(e))$$

$$\overline{\bar{\bar{B}}_{if}}(\beta)=\begin{cases}(\bar{\mu}_{\bar{\bar{B}}_{if}(\beta)}-\sigma_{\bar{\bar{B}}_{if}(\beta)}\sqrt{-2\log\alpha}\ ,\bar{\mu}_{\bar{\bar{B}}_{if}(\beta)}+\sigma_{\bar{\bar{B}}_{if}(\beta)}\sqrt{-2\log\alpha}) & 1<\beta\\ (\bar{\mu}_{\bar{\bar{B}}_{if}(\beta)}-\sigma_{\bar{\bar{B}}_{if}(\beta)}\sqrt{-2\log\alpha}\ ,\bar{\mu}_{\bar{\bar{B}}_{if}(\beta)}+\sigma_{\bar{\bar{B}}_{if}(\beta)}\sqrt{-2\log\alpha}) & 1\ge\beta\end{cases} \quad (65(f))$$

$$\overline{\bar{\bar{\mathcal{A}}}_f}(\beta)=\begin{cases}(\bar{\mu}_{\bar{\bar{\mathcal{A}}}_f(\beta)}-\sigma_{\bar{\bar{\mathcal{A}}}_f(\beta)}\sqrt{-2\log\alpha}\ ,\bar{\mu}_{\bar{\bar{\mathcal{A}}}_f(\beta)}+\sigma_{\bar{\bar{\mathcal{A}}}_f(\beta)}\sqrt{-2\log\alpha}) & 1<\beta\\ (\bar{\mu}_{\bar{\bar{\mathcal{A}}}_f(\beta)}-\sigma_{\bar{\bar{\mathcal{A}}}_f(\beta)}\sqrt{-2\log\alpha}\ ,\bar{\mu}_{\bar{\bar{\mathcal{A}}}_f(\beta)}+\sigma_{\bar{\bar{\mathcal{A}}}_f(\beta)}\sqrt{-2\log\alpha}) & 1\ge\beta\end{cases} \quad (65(g))$$

$$\overline{\bar{\bar{B}}_f}(\beta)=\begin{cases}(\bar{\mu}_{\bar{\bar{B}}_f(\beta)}-\sigma_{\bar{\bar{B}}_f(\beta)}\sqrt{-2\log\alpha}\ ,\bar{\mu}_{\bar{\bar{B}}_f(\beta)}+\sigma_{\overline{\bar{\bar{B}}_f}(\beta)}\sqrt{-2\log\alpha}) & 1<\beta\\ (\bar{\mu}_{\bar{\bar{B}}_f(\beta)}-\sigma_{\bar{\bar{B}}_f(\beta)}\sqrt{-2\log\alpha}\ ,\sigma_{\bar{\bar{B}}_f(\beta)}+\sigma_{\overline{\bar{\bar{B}}_f}(\beta)}\sqrt{-2\log\alpha}) & 1\ge\beta\end{cases} \quad (65(h))$$

Finally,

$$\delta\left(\overline{\bar{\bar{\mathcal{A}}}_{GN}}(\beta)\right)=((\overline{\bar{\bar{\mathcal{A}}}_{GN}}(\beta).(\bar{\bar{\mathcal{A}}}_{t(\beta)},\bar{\bar{\mathcal{A}}}_{it(\beta)},\bar{\bar{\mathcal{A}}}_{if(\beta)},\bar{\bar{\mathcal{A}}}_{f(\beta)})) \quad (66)$$

$$\delta\left(\overline{\bar{\bar{B}}_{GN}}(\beta)\right)=((\overline{\bar{\bar{B}}_{GN}}(\beta).(\bar{\bar{B}}_{t(\beta)},\bar{\bar{B}}_{it(\beta)},\bar{\bar{B}}_{if(\beta)},\bar{\bar{B}}_{f(\beta)})) \quad (67)$$

Where, $\delta\left(\overline{\bar{\bar{\mathcal{A}}}_{GN}}(\beta)\right)$ and $\delta(\overline{B_{GN}}(\beta))$is the absolute value of the variations between the mean intensity of mean and SD of GBTDRINSS and its mean value $\bar{\bar{\mathcal{A}}}_{t(\beta)}$, $\bar{\bar{\mathcal{A}}}_{it(\beta)}$, $\bar{\bar{\mathcal{A}}}_{if(\beta)},\bar{\bar{\mathcal{A}}}_{f(\beta)})$and $\bar{\bar{B}}_{t(\beta)}$, $\bar{\bar{B}}_{it(\beta)}$, $\bar{\bar{B}}_{if(\beta)},\bar{\bar{B}}_{f(\beta)}$. After the $\beta -$ enhancement operation, the membership set of GBTDRINI in which I comes

more distinct which is suitable for CXR images segmentation tasks, as it removes the noise and retains detailed information.

3.5 IMAGE SEGMENTATION

3.5.1 Segmentation on NI domain

For the segmentation process, K- means clustering analysis on NS is determined. The clustering can classify similar sample points into the same group. Assume, $I = I_a, m = 1,2, \dots n$ be image sample and x_a be a simple in a $d-$ dimensional space. The problem of clustering is to identify the partition $R = R_1, R_2, \dots, R_k$, which satisfies the Eq. (68)

$$I = \cup_{a=1}^{k} R_a \quad (68)$$

$R_a \neq \Phi$ for $a = 1, 2, .., k$

$R_a \cap R_b \neq \Phi$ for $a, b = 1, 2, .., k,\ a \neq b$

Among clustering methods, the K-means algorithm is widely used. It is important to define an objective function for a clustering analysis method. Each cluster should be as compact as possible. The objective function of K-means is defined as

$$Z_R = \sum_{b=1}^{k} \sum_{a=1}^{l_b} \|D_a - V_b\| \quad (69)$$

In Eq. (69)V_b is the centre of the b^{th} cluster, k is the total number of clusters and l_b is the number of pixels in theb^{th} cluster. The condition towards the minimum Z_R

$$Z_b = \frac{1}{l_b} \sum_{D_a \epsilon R_b} I_a \quad (70)$$

In Eq. (70), l_b is represented as the number of elements in clusters R_b.

A new clustering method is defined for the NS and it deals with $\bar{P}_{NS}(a, b)$, the NS after the $\alpha-$ mean and $\beta-$ enhancement by implementing $\alpha-$mean and $\beta-$ enhancement operations. On considering the effect of indeterminacy, the two set$T$ and I are composed into a new value of clustering which is illustrated in Eq. (71)

$$I(a, b) = \begin{cases} T(a, b), & I(a, b) \leq K \\ \overline{T_K}(a, b), & I(a, b) > K \end{cases} \quad (71)$$

The new clustering technique for the NS, i.e., $K - means$ clustering is applied to the subset T. The new objective operation $T_K - means$ is constructed in Eq. (72(a-b))

$$Z_{T_R} = \sum_{q=1}^{G} \sum_{a=1}^{Y} \sum_{b=1}^{W} \left\| I(a, b) - Z_q \right\|^2 \quad (72(a))$$

$$Z_q = \frac{1}{l_q} \sum_{D(a,b) \in R_q} I(a, b) \quad (72(b))$$

Finally, the image is segmented using the proposed $K-$ means clustering method for the NS domain.

3.5.2 Segmentation on BTDRINI domain

For the segmentation process, K- means clustering analysis on BTDRINI is determined. A new clustering method is defined for the BTDRINSS and it deals with $\overline{\ddot{A}_{B_i T}}(a_1, a_2, a_2, a_3, a_4\ ;\ p_{B_i T_K}, q_{B_i T_K}, r_{B_i T_K}, s_{B_i T_K})$, the NS after the $\alpha-$ mean and $\beta-$ enhancement by implementing $\alpha-$mean and $\beta-$ enhancement operations. On considering the effect of indeterminacy, there are composed into a new value of clustering which is illustrated in Eq. (73 (a-h))

Table 6 Segmentation on BTDRINI domain

Positive Degree of Truth-Membership	**Negative Degree of Truth-Membership**
$I\left(\overline{T_K^{+}}(x)\right) = \begin{cases} p_{B_i T_K} \frac{x - a_1}{a_2 - a_1} a_1 \leq x < a_2 \\ p_{B_i T_K} a_2 \leq x \leq a_3 \\ p_{B_i T_K} \frac{a_4 - x}{a_4 - a_3} a_3 < x \leq a_4 \\ 0 \quad otherwise \end{cases}$ (73(a))	$I\left(\overline{T_K^{-}}(x)\right) = \begin{cases} p_{B_i T_K} \frac{a_1 - x}{a_2 - a_1} a_1 \leq x < a_2 \\ -p_{B_i T_K} a_2 \leq x \leq a_3 \\ p_{B_i T_\beta} \frac{x - a_4}{a_4 - a_3} a_3 < x \leq a_4 \\ 0 \quad otherwise \end{cases}$ (73(b))
Positive degree of Indeterminate toward Truth Membership	**Negative degree of indeterminate towards truth membership**
$I\left(\overline{I_{T_K}^{+}}(x)\right) = \begin{cases} q_{B_i T_K} \frac{x - a_1}{a_2 - a_1} a_1 \leq x < a_2 \\ q_{B_i T_K} a_2 \leq x \leq a_3 \\ q_{B_i T_K} \frac{a_4 - x}{a_4 - a_3} a_3 < x \leq a_4 \\ 0 \quad otherwise \end{cases}$ ((73(c))	$I\left(\overline{I_{T_K}^{-}}(x)\right) = \begin{cases} q_{B_i T_K} \frac{a_1 - x}{a_2 - a_1} a_1 \leq x < a_2 \\ -q_{B_i T_K} a_2 \leq x \leq a_3 \\ q_{B_i T_K} \frac{x - a_4}{a_4 - a_3} a_3 < x \leq a_4 \\ 0 \quad otherwise \end{cases}$ (73(d))
Positive Degree Of Indeterminate Toward Falsity	**Negative Degree Of Indeterminate toward Falsity**

$$I\left(\overline{I_{F_K}^{+}}\right)(x)=\begin{cases}\frac{a_2-x+r_{B_iT_K}(x-a_1)}{a_2-a_1}a_1 \le x<a_2\\ r_{B_iT_K}a_2 \le x\le a_3\\ \frac{x-a_3+r_{B_iT_K}(a_4-x)}{a_4-a_3}a_3<x\le a_4\\ 1 \quad otherwise\end{cases} \quad (73(e))$$

$$I\left(\overline{I_{F_K}^{-}}\right)(x)=\begin{cases}\frac{x-a_2+r_{B_iT_K}(a_1-x)}{a_2-a_1}a_1 \le x<a_2\\ -r_{B_iT_K}a_2 \le x\le a_3\\ \frac{a_3-x+r_{B_iT_K}(x-a_4)}{a_4-a_3}a_3<x\le a_4\\ -1 \quad otherwise\end{cases} \quad (73(f))$$

Positive degree of Falsity membership | **Negative degree of Falsity membership**

$$I(F_K^{+}(x))=\begin{cases}\frac{a_2-x+s_{B_iT_\beta}(x-a_1)}{a_2-a_1}a_1 \le x<a_2\\ s_{B_iT_\beta}a_2 \le x\le a_3\\ \frac{x-a_3+s_{B_iT_\beta}(a_4-x)}{a_4-a_3}a_3<x\le a_4\\ 1 \quad otherwise\end{cases} \quad (73(g))$$

$$I(F_K^{+}(x))=\begin{cases}\frac{x-a_2+s_{B_iT_K}(a_1-x)}{a_2-a_1}a_1 \le x<a_2\\ -s_{B_iT_K}a_2 \le x\le a_3\\ \frac{a_3-x+s_{B_iT_K}(x-a_4)}{a_4-a_3}a_3<x\le a_4\\ -1 \quad otherwise\end{cases} \quad (73(h))$$

The new clustering technique for the BTDRINSS, i.e., $K-means$ clustering is applied to the subset $\overline{T_K^{+}}(x),\overline{T_K^{-}}(x),\overline{I_{T_K}^{+}}(x),\overline{I_{FT_K}^{-}}(x),\overline{I_{F_K}^{-}}(x),\overline{I_{F_K}^{-}}(x),\overline{F_K^{+}}(x)$ and $\overline{F_K^{-}}(x)$

The new objective operation $\overline{\ddot{\mathcal{A}}_{B_iT}}\ (K)$ $means$ is constructed in Eq. (74-75)

$$Z_{\overline{\ddot{\mathcal{A}}_{B_iT}}\ (K)}=\sum_{q=1}^{K}\left\|I\left(\overline{T_K^{+}}(x),\overline{T_K^{-}}(x),\overline{I_{T_K}^{+}}(x),\overline{I_{FT_K}^{-}}(x),\overline{I_{F_K}^{-}}(x),\overline{I_{F_K}^{-}}(x),\overline{F_K^{+}}(x)\right)\overline{F_K^{-}}(x)-Z_q\right\|^2 (74)$$

$$Z_q=\frac{1}{l_q}\sum_{I(a_1,a_2,a_2,a_3,a_4\,;p_{B_iT_K},q_{B_iT_K},r_{B_iT_K},s_{B_iT_K})\in R_q}I(\overline{\ddot{\mathcal{A}}_{B_iT}}\ (K)) (75)$$

Finally, the image is segmented using the $K-$ means clustering method for the BTDRINSS domain.

3.5.3 Segmentation on GBTDRINI domain

For the segmentation process, K- means clustering analysis on GBTDRINI is determined. A new clustering method is defined for the BTDRINSS and it deals with $\overline{\bar{\mathcal{A}}_{GN}}(K)=\overline{\bar{\mathcal{A}}_{t_K}},\overline{\bar{\mathcal{A}}_{\iota t_K}},\overline{\bar{\mathcal{A}}_{\iota f_K}},\overline{\bar{\mathcal{A}}_{f_K}}$ and $\overline{B_{GN}}(K)=\overline{\bar{B}_{t_K}},\overline{\bar{B}_{\iota t_K}},\overline{\bar{B}_{\iota f_K}},\overline{\bar{B}_{f_K}}$, the NS after the $\alpha-$ mean and $\beta-$ enhancement by implementing $\alpha-$mean and $\beta-$ enhancement operations. On considering the effect of indeterminacy, there are composed into a new value of clustering which is illustrated in Eq. (76(a-h))

$$\overline{\bar{\mathcal{A}}_t}(K)=\begin{cases}(\bar{\mu}_{\bar{\mathcal{A}}_t(K)}-\sigma_{\bar{\mathcal{A}}_t(K)}\sqrt{-2\log\alpha}\ ,\bar{\mu}_{\bar{\mathcal{A}}_t(K)}+\sigma_{\bar{\mathcal{A}}_t(K)}\sqrt{-2\log\alpha}) & 1<K\\ (\bar{\mu}_{\bar{\mathcal{A}}_t(K)}-\sigma_{\bar{\mathcal{A}}_t(K)}\sqrt{-2\log\alpha}\ ,\bar{\mu}_{\bar{\mathcal{A}}_t(K)}+\sigma_{\bar{\mathcal{A}}_t(K)}\sqrt{-2\log\alpha}) & 1\ge K\end{cases} \quad (76(a))$$

$$\overline{\bar{B}_t}(K)=\begin{cases}(\bar{\mu}_{\bar{B}_t(K)}-\sigma_{\bar{B}_t(K)}\sqrt{-2\log\alpha}\ ,\bar{\mu}_{\bar{B}_t(K)}+\sigma_{\bar{B}_t(K)}\sqrt{-2\log\alpha}) & 1<K\\ (\bar{\mu}_{\bar{B}_t(K)}-\sigma_{\bar{B}_t(K)}\sqrt{-2\log\alpha}\ ,\bar{\mu}_{\bar{B}_t(K)}+\sigma_{\bar{B}_t(K)}\sqrt{-2\log\alpha}) & 1\ge K\end{cases} \quad (76(b))$$

$$\overline{\bar{\mathcal{A}}_{\iota t}}(K)=\begin{cases}(\bar{\mu}_{\bar{\mathcal{A}}_{it}(K)}-\sigma_{\bar{\mathcal{A}}_{it}(K)}\sqrt{-2\log\alpha}\ ,\bar{\mu}_{\bar{\mathcal{A}}_{it}(K)}+\sigma_{\bar{\mathcal{A}}_{it}(K)}\sqrt{-2\log\alpha}) & 1<K\\ (\bar{\mu}_{\bar{\mathcal{A}}_{it}(K)}-\sigma_{\bar{\mathcal{A}}_{it}(K)}\sqrt{-2\log\alpha}\ ,\bar{\mu}_{\bar{\mathcal{A}}_{it}(K)}+\sigma_{\bar{\mathcal{A}}_{it}(K)}\sqrt{-2\log\alpha}) & 1\ge K\end{cases} (76(c))$$

$$\overline{\bar{B}_{\iota t}}(K)=\begin{cases}(\bar{\mu}_{\bar{B}_{it}(K)}-\sigma_{(\bar{B}_{it}(K)}\sqrt{-2\log\alpha}\ ,\bar{\mu}_{\bar{B}_{it}(K)}+\sigma_{\bar{B}_{it}(K)}\sqrt{-2\log\alpha}) & 1<K\\ (\bar{\mu}_{\bar{B}_{it}(K)}-\sigma_{\bar{B}_{it}(K)}\sqrt{-2\log\alpha}\ ,\bar{\mu}_{\bar{B}_{it}(K)}+\sigma_{\bar{B}_{it}(K)}\sqrt{-2\log\alpha}) & 1\ge K\end{cases} (76(d))$$

$$\overline{\bar{\mathcal{A}}_{\iota f}}(K)=\begin{cases}(\bar{\mu}_{\bar{\mathcal{A}}_{if}(K)}-\sigma_{\bar{\mathcal{A}}_{if}(K)}\sqrt{-2\log\alpha}\ ,\bar{\mu}_{\bar{\mathcal{A}}_{if}(K)}+\sigma_{\bar{\mathcal{A}}_{if}(K)}\sqrt{-2\log\alpha}) & 1<K\\ (\bar{\mu}_{\bar{\mathcal{A}}_{if}(K)}-\sigma_{\bar{\mathcal{A}}_{if}(K)}\sqrt{-2\log\alpha}\ ,\bar{\mu}_{\bar{\mathcal{A}}_{if}(K)}+\sigma_{\bar{\mathcal{A}}_{if}(K)}\sqrt{-2\log\alpha}) & 1\ge K\end{cases} (76(e))$$

$$\overline{\bar{B}_{\iota f}}(K)=\begin{cases}(\bar{\mu}_{\bar{B}_{if}(K)}-\sigma_{\bar{B}_{if}(K)}\sqrt{-2\log\alpha}\ ,\bar{\mu}_{\bar{B}_{if}(K)}+\sigma_{\bar{B}_{if}(K)}\sqrt{-2\log\alpha}) & 1<K\\ (\bar{\mu}_{\bar{B}_{if}(K)}-\sigma_{\bar{B}_{if}(K)}\sqrt{-2\log\alpha}\ ,\bar{\mu}_{\bar{B}_{if}(K)}+\sigma_{\bar{B}_{if}(K)}\sqrt{-2\log\alpha}) & 1\ge K\end{cases} (76(f))$$

$$\overline{\bar{\mathcal{A}}_f}(K)=\begin{cases}(\bar{\mu}_{\bar{\mathcal{A}}_f(K)}-\sigma_{\bar{\mathcal{A}}_f(K)}\sqrt{-2\log\alpha}\ ,\bar{\mu}_{\bar{\mathcal{A}}_f(K)}+\sigma_{\bar{\mathcal{A}}_f(K)}\sqrt{-2\log\alpha}) & 1<K\\ (\bar{\mu}_{\bar{\mathcal{A}}_f(K)}-\sigma_{\bar{\mathcal{A}}_f(K)}\sqrt{-2\log\alpha}\ ,\bar{\mu}_{\bar{\mathcal{A}}_f(K)}+\sigma_{\bar{\mathcal{A}}_f(K)}\sqrt{-2\log\alpha}) & 1\ge K\end{cases} (76(g))$$

$$\overline{\bar{B}_f}(K)=\begin{cases}(\bar{\mu}_{\bar{B}_f(K)}-\sigma_{\bar{B}_f(K)}\sqrt{-2\log\alpha}\ ,\bar{\mu}_{\bar{B}_f(K)}+\sigma_{\bar{B}_f(K)}\sqrt{-2\log\alpha}) & 1<K\\ (\bar{\mu}_{\bar{B}_f(K)}-\sigma_{\bar{B}_f(K)}\sqrt{-2\log\alpha}\ ,\sigma_{\bar{B}_f(K)}+\sigma_{\bar{B}_f(K)}\sqrt{-2\log\alpha}) & 1\ge K\end{cases} (76(h))$$

The new clustering technique for the BTDRINSS, i.e., $K-means$ clustering is applied to the subset $\bar{\bar{\mathcal{A}}}_{t(K)}$, $\bar{\bar{\mathcal{A}}}_{it(K)}$, $\bar{\bar{\mathcal{A}}}_{if(K)}$, $\bar{\bar{\mathcal{A}}}_{f(K)}$ and $\bar{\bar{B}}_{t(K)}$, $\bar{\bar{B}}_{it(K)}$, $\bar{\bar{B}}_{if(K)}$, $\bar{\bar{B}}_{f(K)}$. The new objective operation of $\overline{\bar{\bar{\mathcal{A}}}_{GN}}(K)$ and $\overline{\bar{\bar{B}}_{GN}}(K)$is constructed in Eq. (77-78)

$$Z_{\overline{\bar{\bar{\mathcal{A}}}_{GN}}(K)} = \sum_{q=1}^{K} \left\| I\left(\bar{\bar{\mathcal{A}}}_{t(K)}, \bar{\bar{\mathcal{A}}}_{it(K)}, \bar{\bar{\mathcal{A}}}_{if(K)}, \bar{\bar{\mathcal{A}}}_{f(K)}\right) \right\|^2 (77)$$

$$Z_{\overline{\bar{\bar{B}}_{GN}}(K)} = \sum_{q=1}^{K} \left\| I\left(\bar{\bar{B}}_{t(K)}, \bar{\bar{B}}_{it(K)}, \bar{\bar{B}}_{if(K)}, \bar{\bar{B}}_{f(K)}\right) \right\|^2 (78)$$

$$Z_q = \frac{1}{l_q} \sum_{I(\left(\bar{\bar{\mathcal{A}}}_{t(K)}, \bar{\bar{\mathcal{A}}}_{it(K)}, \bar{\bar{\mathcal{A}}}_{if(K)}, \bar{\bar{\mathcal{A}}}_{f(K)}\right)) \in R_q} I(\overline{\bar{\bar{\mathcal{A}}}_{GN}}(K)) (79)$$

$$Z_E = \frac{1}{l_e} \sum_{I(\left(\bar{\bar{B}}_{t(K)}, \bar{\bar{B}}_{it(K)}, \bar{\bar{B}}_{if(K)}, \bar{\bar{B}}_{f(K)}\right)) \in R_e} I(\overline{\bar{\bar{\mathcal{A}}}_{GN}}(K)) (79(a))$$

Finally, the image is segmented using the $K-$ means clustering method for the GBTDRINSS domain.

3.6 IMAGE CLASSIFICATION

The segmented Ψ- T images are then trained by taking the benefits of enhanced features. The training is processed in three phases which is depicted in figure 3.

Stage 1: Initially, each input CXR images is resized into three different scales. This is done using average pooling and it forms image pyramid and then each scaled version is travelled to the convolutional layers in ResNet50 model.

Stage 2: Detection task is done using DL model i.e., Res-Net 50. The ResNet50 is a typical deep residual network whose structure mainly composed of50 layers, including 49 convolutional layers and one fully connected layer. Among them,49 convolutional layers can be divided into 5 parts, the first part of building blocks. Each bottleneck building block is composed of several convolutionallayers, batch normalizations, and rectified linear unit (ReLU) activation functions. At first, ResNet-50 performed convolution operation on the input,followed by 4 residual blocks, and finally performed full connection operation to achieve classification tasks. The residual building block can be expressed by the following Eq. (80),

$$y = F(x) + x \quad (80)$$

Where, $F(x)$ is called the residual function, and x and y are the input and output parameters of the residual function, respectively. It is worth noting that y is actually the x of the next residual block.In thisframework, 10different pre-trained weights of the ResNet50 model to carry out transfer learning on the CXR images. The architecture for proposed ResNet 50 is presented in Table 7.

There are a series of convolutional ($conv$) layers in ResNet50 architecture. First $conv$ layer is made of 7×7 kernel size and 64 different kernels with a stride size of 2. Then 3×3 max pooling with the stride of size 2 is applied. In the next convolution, there are three $conv$ layers($1 \times 1, 64\ kernels$, $(3 \times 3, 64\ kernels)$ and $(1 \times 1, 256\ kernels)$ respectively and these three layers are repeated in total 3 times. In the same process, three $conv$ layers $(1 \times 1, 128\ kernels), (3 \times 3, 128\ kernels)$ and $(1 \times 1, 512\ kernels)$ respectively are repeated four times three $conv$ layers$(1 \times 1, 256\ kernels)$, $(3 \times 3, 256\ kernels)$ and $(1 \times 1,1024\ kernels)$ respectively are repeated six times and another three conv layers (1 × 1, 512 kernels), $(3 \times 3, 512\ kernels)$ and $(1 \times 1, 2048\ kernels)$ respectively are repeated3 times. Then average pooling (avg. pool) is applied. Most of the hidden layers use Batch Normalization, and ReLU followed by a conv layer

Table 7. ResNet50 structure

Layer Name	Output Size	50 – Layers
$conv\ 1$	$112 * 112$	$7 * 7, 64$, stride 2
$conv\ 2\_x$	$56 * 56$	$3 * 3$ max pool, stride 2
		$[1 * 1, 64$ $3 * 3, 64$ $1 * 1, 256\ ] * 3$
$conv\ 3\_x$	$28 * 28$	$[1 * 1, 128$

		$3*3, 128$ $1*1, 512\ ]*4$
$conv\ 4\_x$	$14*14$	$[1*1, 256$ $3*3, 256$ $1*1, 1024\ ]*6$
$conv\ 5\_x$	$7*7$	$[1*1, 512$ $3*3, 512$ $1*1, 2048\ ]*3$
$FC\ 1$	$1*1$	Average Pool $In\_Features\ =\ 2048;$ $Out\_Features\ =\ 2048$
$FC\ 2$	$1*1$	Drop out = 0.5 $In\_Features\ =\ 2048;$ $Out\_Features\ =\ 2048$
$FC\ 3$	$1*1$	ReLu, dropout = 0.5 $In\_Features\ =\ 2048;$ $Out\_Features\ =\ 2048$

The Constructed ResNet-50 model is fine-tuned by replacing this FC layer with a set of FC layers. The first FC layer has 2048 out-features, then dropout with a probability of 0.5 is applied. The second FC layer is the same as the first fc layer. After the second FC layer, ReLU and dropout with probability 0.5 are applied. The final FC layer consists of 2048 in featuresand only 2 out-features for the classification of different lung diseases types. The figure 2depicts the structure of ResNet-50 Model.

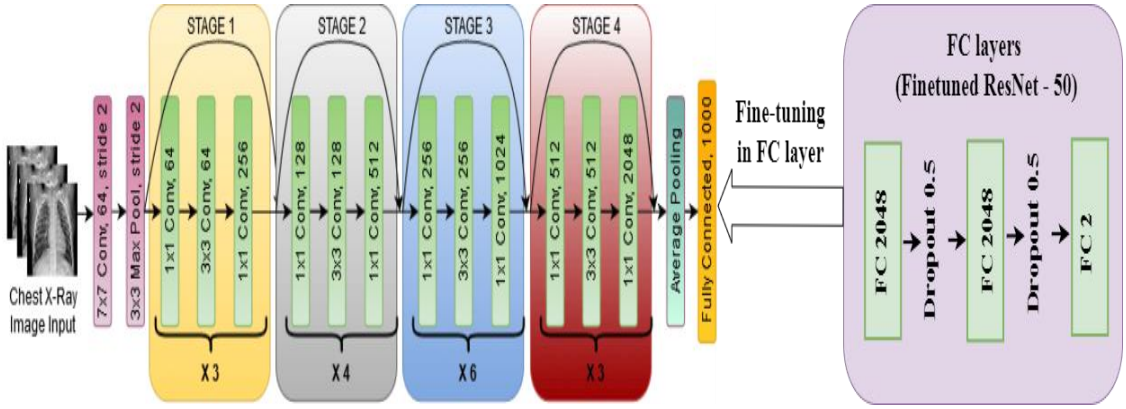

Figure 2 Constructed ResNet- 50 Structure

Stage 3: The outcomes are classified from the constructed classifier to determine the types of lung diseases.

Algorithm: CNSDL Model

Input: CXR images Im_X , NS domain

Output: Types of Lung disease classification

For each image Im_X in dataset

Convert to gray scale image (H)

{

If (domain is NS)

Transform the image into a NS domain using Eqs. (17-22)

Compute the entropy of the NS domain membership i.e., E_T , E_I and $E_F$using Eq. (28-29(c))

Apply α- mean operation onP_{NS}using Eq. (35-41)

Perform$\beta - enhancement$ operations for P_{NS} i.e., $P'_{NS}(\beta)$using Eqs. (42-48)

Apply the $K-$means clustering to the NI domain subset using Eq. (68- 72(b))

Classify the segmented images using fine-tuned ResNet 50 structure as given in table 7.

Identify the resultant class as lung diseases types i.e., Normal, Viral Pneumonia, Bacterial Pneumonia, Covid -19)

}

Else If (domain is BTDRINSS)

{

Transform the image into a BTDRINSS domain using Eqs. (23-24(h))

Compute the entropy of the BTDRINSS domain membership i.e., E_T+, E_T−, E_{I_T}+ ,

$E_{I_T}-$, $E_{I_F}+$, $E_{I_F}-$, E_F+, E_F- using Eq. (30-31(h))

Apply α- mean operation onBTDRINI i.e., $\overline{\ddot{\mathcal{A}}_{B_iT}}(\alpha)$using Eq. (49-51)

Perform β- enhancements operation onBTDRINI, i.e., $\ddot{\mathcal{A}}_{B_iT}{}'(\beta)$ isusing Eqs. (52-55)

Apply the $K-$ means clustering to the BTDRINI domain subset i.e., using Eq. (73(a) - 75)

Classify the segmented images using fine-tuned ResNet 50 structure as given in table 7.

Identify the resultant class as lung diseases types i.e., Normal, Viral Pneumonia, Bacterial, Pneumonia, Covid -19)

}

Else If (domain is GBTDRINSS)

{

Transform the image into a GBTDRINSS domain using Eqs. (25-27(d))

Compute the entropy of the GBTDRINSS domain memberships i.e.,$E_{\bar{\mathcal{A}}_t}$, $E_{\bar{\mathcal{A}}_{it}}, E_{\bar{\mathcal{A}}_{if}}, E_{\bar{\mathcal{A}}_f}, E_{\bar{\bar{B}}_t}, E_{\bar{\bar{B}}_{it}}, E_{\bar{\bar{B}}_{if}}$ and using Eq. (32-34(h))

Apply α- mean operation on GBTDRINSS i.e., $\overline{\bar{\bar{\mathcal{A}}}_{GN}}(\alpha)$ and $\overline{B_{GN}}(\alpha)$ using Eq. (56-60)

Perform β- enhancements operation on GBTDRINS i.e., $\overline{\bar{\bar{\mathcal{A}}}_{GN}}(\beta)$ and $\overline{B_{GN}}(\beta)$using Eqs. (61-67)

Apply the $K-$ means clustering to the GBTDRINI domain subset using Eq. (76(a)-79(a))

Classify the segmented images using fine-tuned ResNet 50 structure as given in table 7.

Identify the resultant class as lung diseases types i.e., Normal, Viral Pneumonia, Bacterial Pneumonia, Covid -19)

}

End }

End}

End }

4. RESULT AND DISCUSSION

In this section, the efficiency of the CNSDL model is examined by implementing it in MATLAB 2019a using the CXR images diseases types which is discussed in Section 3.1. For the experimental purposes, 70% of images are taken for training and the remaining 30% are taken for testing of the NSDL model from each categories of lung diseases using both CXR images. Further a comparative analysis is carried out for different models like Intuitionistic Fuzzy Sets (IFS), Neutrosophic Sets (NSS), BTDRINSS and GBTDRINSS in order to understand the improvement of the techniques considered for the lung cancer detection. This comparison is divided into three performance stages i.e., which is illustrated below.

4.1.Entropy

Entropy quantifies the image information content i.e., evaluation of the distribution of the intensity ranges. The more detailed information indicates higher clarity of the image leading to higher entropy value. To improve the robustness and effectiveness of the IFS, NSS, BTDRINSS and GBTDRINSS domain of CXR images, the T, I and F of respective domains are operated using α and β operations. The entropy of these images signifies how much thedetailed images are extracted. Table 8 portrays an increase in entropy values of the X-ray images after alpha and beta operation for three different domain.

Table 8 Determined Entropy Values for different NI domain with CXR images

Techniques	Entropy
IFS	**19.190**
NS	**22.869**
BTDRINSS	**24.789**
GBTDRINSS	**31.856**

From the above table, it is analyzed that the Entropy values of GBTDRINSS is higher than IFS, NSS and BTDRINSS. For instances, the GBTDRINSS domain is 28.50% of BTDRINS, 39.29% of NSS, and 66% of IFS, which provides the higher robustness and efficiency of theGBTDRINSSfor CXR images using α and β operations.

4.2. Peak Signal-to-Noise Ratio (PSNR): The qualitative way to analyse the enhanced image isdone using PSNR. It is definedas the ratio between the maximum possible value(power) of a signal and the power of distorting noise thataffects the quality of its representation and is measuredin decibels. The higher the PSNR value indicates better the image quality and hence after beta enhancement the PSNR values holds up to 75.15 dB when compared to original X-ray image The mathematical representation ofPSNR is defined using Equations (81 (a)-(b)).

$PSNR = 26log_{10}\left(\frac{max_f}{\sqrt{MSE}}\right)$
(81(a))
$MSE = \frac{1}{m*n}\sum_0^{m=1}\sum_0^{n=1}\|f(I,j) - g(I,j)\|^2$(81(b))
The Eq. (81(b)), max_f represents the maximum pixel intensity value of the image. In this analysis, the max_f value used is 255. Here, f and g are two $m \times n$ images where one of the images is considered a noisy approximation compared to the other.The table 9 provides the comparison of PSNR and MSE for proposed NS domains.

Table 9 Values of PSNR and MSE parameters of the enhanced (NS) images

Techniques	PSNR	MSE
IFS	**53.35**	**0.061**
NS	**59.19**	**0.053**
BTDRINSS	**62.84**	**0.037**
GBTDRINSS	**75.96**	**0.019**

The table 9 provides the values of PSNRand MSE values of IFS, NSS, BTDRINSS and GBTDRINSS. The PSNR and MSE values of GBTDRINSS is75.96db and 0.019 respectively, which is comparatively higher that the IFS, NSS and BTDRINSS Since, the GBTDRINIdomain provides the higher PSNR values and lower MSE values, as it indicates the better image quality and enhancement.

4.3. Performance Comparison of Proposed with Existing Methods for classification stage (classifier)

The evaluation metrics used to measure the success of the proposed and existing models by respective classifierare briefly illustrated below in Eq. (82(a-d))

4.3.1 Accuracy: The proportion of lung disease cases correctly classified is calculated as the number of cases correctly classified in each class divided by the total number of cases

$Accuracy = \frac{TP+TN}{TP+TN+FP+FN}$

(82(a))

TP (True Positive) result indicates that the model correctly identified lung diseases e.g., pneumonia is classified as pneumonia. TN (True Negative) outcome represents that the model accurately classifies other lung diseases as others e.g., other diseases except pneumonia is classified as others. FP (False Positive) outcome indicates that the model incorrectly classified true cases of lung disease, such as pneumonia as other diseases. FN (False Negative) outcome represents that the model inaccurately classifies the other diseases as actual e.g., other diseases are classified as pneumonia.

4.3.2 Precision: It is the proportion of correctly labelled cases of lung illnesses at both the TP and FP rates.

$Precision = \frac{TP}{TP+FP}$(82(b))

4.3.3 Recall: It is the ratio of exactly classified categories of lung diseases cases at TP and FN rates for all classes.

$Recall = \frac{TP}{TP+FN}$(82(c))

4.3.4 F1-Score: It is the average of the two measures of accuracy precisions and recall

$F1 - score = 2 \times \frac{Precision \cdot Recall}{Precision+Recall}$(82(d))

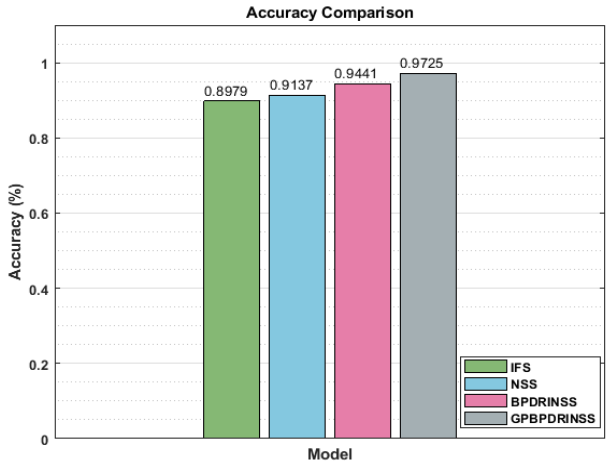

Figure 3 Accuracy Evaluation

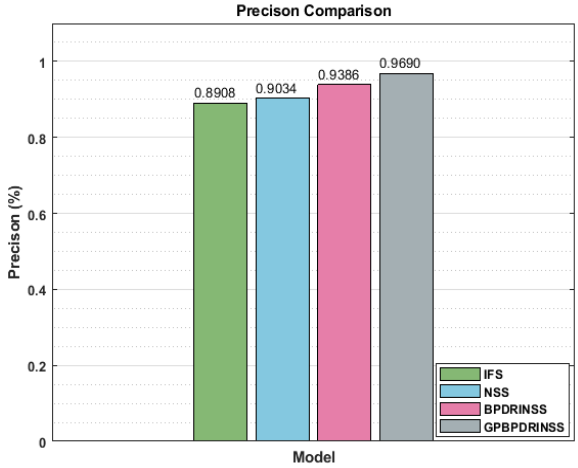

Figure 4 Precision Evaluation

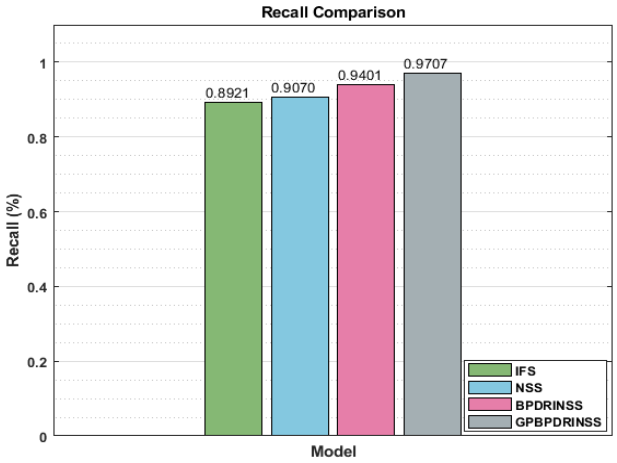

Figure 5 Recall Evaluation

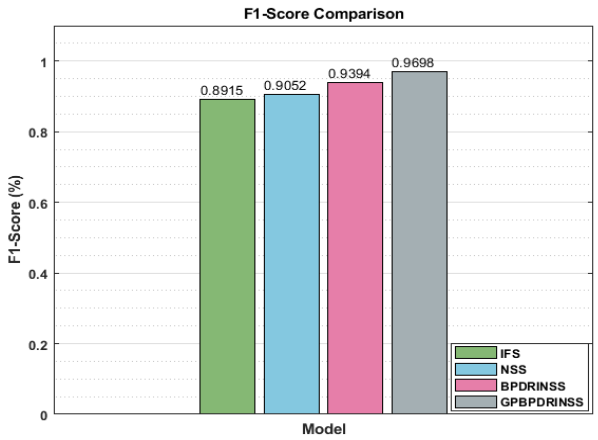

Figure 6 F1-Score Evaluation

The above figure 3 -6 displays the efficacy of various models on the CXR databases for lung diseases identification using different performance metrics like accuracy, precision, recall and F1-Score. It declares that the success rate of the GBTDRINSS model regarding accuracy, precision, recall, and F-score is greater than that of all other earlier models because it enhances themaximizes the accuracy of recognizing the lung diseases by pre-processing, segmentation and classification effectively compared to the other earlier models.Accordingly, it is understood that the accuracy of the GBTDRINSS is8.31%, 6.43%, and 3.01% superior to the IFS, NSS and BTDRINSS. The precision of the GBTDRINSS is 8.78%, 7.26%, and 3.24% superior to the IFS, NSS and BTDRINSS models. The recall of the GBTDRINSS is 8.81%, 7.02% and 3.25% superior to the IFS, NSS and BTDRINSS models. Also, the F-score of the GBTDRINSS is 8.78%, 7.14% and 3.24% superior to the IFS, NSS and BTDRINSS models.

5. CONCLUSION

In this paper, CNSDL model is developed for lung diseases. This method effectively resolves the spatial pixel data issues due to noise and artifacts which play a vital role in many real-time applications. In this model, BTDRINS and GBTDRINSS is developed and employed along with the original NS for the prediction tasks. The suggested model is categorized into three stages. Initially, the input CXR images are converted to three NS domain with T, F and I set images individually which reduces the fuzziness and retain more significant information for feature extraction of the opacity to distinguish the types of lung diseases. The entropy in three NS domain is applied to evaluate the indeterminacy. Then, the two operations like α −mean and β −enhancement operations are used to reduce the set indeterminacy to enhance the image edges to improve accuracy. In addition, $K-$ means clustering method is utilized for the image segmentation tasks. Finally, the enhanced image features are given as input to the ResNet 50to train and test for the type of lung diseases. The test experimental outcomes show that the proposed GBTDRINSS provides the accuracy of 97.25% on lung diseases prediction compared to the other existing models.

REFERENCES

1. Cruz, A. A. (2007). Global surveillance, prevention and control of chronic respiratory diseases: a comprehensive approach. World Health Organization.
2. Marciniuk, D. D., & Schraufnagel, D. E. (2017). The global impact of respiratory disease. European Respiratory Society.
3. Mridha, M. F., Prodeep, A. R., Hoque, A. S. M., Islam, M., Lima, A. A., Kabir, M. M., ... &Watanobe, Y. (2022). A Comprehensive Survey on the Progress, Process, and Challenges of Lung Cancer Detection and Classification. Journal of Healthcare Engineering, 2022.
4. Collins, L. G., Haines, C., Perkel, R., &Enck, R. E. (2007). Lung cancer: diagnosis and management. American family physician, 75(1), 56-63.

5. Vieira, P., Sousa, O., Magalhães, D., Rabêlo, R., & Silva, R. (2021). Detecting pulmonary diseases using deep features in X-ray images. Pattern Recognition, 119, 108081.
6. Liang, C. H., Liu, Y. C., Wu, M. T., Garcia-Castro, F., Alberich-Bayarri, A., & Wu, F. Z. (2020). Identifying pulmonary nodules or masses on chest radiography using deep learning: external validation and strategies to improve clinical practice. Clinical radiology, 75(1), 38-45.
7. Chouhan, V., Singh, S. K., Khamparia, A., Gupta, D., Tiwari, P., Moreira, C., ... & De Albuquerque, V. H. C. (2020). A novel transfer learning based approach for pneumonia detection in chest X-ray images. Applied Sciences, 10(2), 559.
8. Rajaraman, S., & Antani, S. K. (2020). Modality-specific deep learning model ensembles toward improving TB detection in chest radiographs. IEEE Access, 8, 27318-27326.
9. Tiwari, S. K., Walia, N., Singh, H., & Sharma, A. (2015). Effective analysis of lung infection using fuzzy rules. International Journal of Bio-Science and Bio-Technology, 7(6), 85-96.
10. Wang, H., Smarandache, F., Sunderraman, R., & Zhang, Y. Q. (2005). interval neutrosophic sets and logic: theory and applications in computing: Theory and applications in computing (Vol. 5). Infinite Study.
11. Wu, C., Luo, C., Xiong, N., Zhang, W., & Kim, T. H. (2018). A greedy deep learning method for medical disease analysis. IEEE Access, 6, 20021-20030.
12. Kieu, S. T. H., Bade, A., Hijazi, M. H. A., &Kolivand, H. (2020). A survey of deep learning for lung disease detection on medical images: state-of-the-art, taxonomy, issues and future directions. Journal of imaging, 6(12), 131.
13. Bharati, S., Podder, P., & Mondal, M. R. H. (2020). Hybrid deep learning for detecting lung diseases from X-ray images. Informatics in Medicine Unlocked, 20, 100391.
14. Hashmi, M. F., Katiyar, S., Keskar, A. G., Bokde, N. D., &Geem, Z. W. (2020). Efficient pneumonia detection in chest x-ray images using deep transfer learning. Diagnostics, 10(6), 417.
15. Wang, W., Li, Y., Li, J., Zhang, P., & Wang, X. (2021). Detecting COVID-19 in chest x-ray images via MCFF-Net. Computational Intelligence and Neuroscience, 2021, 1-8.
16. Zhang, D., Ren, F., Li, Y., Na, L., & Ma, Y. (2021). Pneumonia detection from chest X-ray images based on convolutional neural network. Electronics, 10(13), 1512.
17. Kim, S., Rim, B., Choi, S., Lee, A., Min, S., & Hong, M. (2022). Deep learning in multi-class lung diseases' classification on chest X-ray images. Diagnostics, 12(4), 915.
18. Abdel-Basset, M., Mostafa, N. N., Sallam, K. M., Elgendi, I., &Munasinghe, K. (2022). Enhanced COVID-19 X-ray image preprocessing schema using type-2 neutrosophic set. Applied Soft Computing, 123, 108948.
19. Karataş, E., & Ozturk, T. Y. (2022). An Application Method for the use of Neutrosophic Soft Mappings in Decision-Making the Diagnosis of Covid-19 and Other Lung Diseases. Process Integration and Optimization for Sustainability, 1-14.
20. Ieracitano, C., Mammone, N., Versaci, M., Varone, G., Ali, A. R., Armentano, A., ... & Morabito, F. C. (2022). A fuzzy-enhanced deep learning approach for early detection of Covid-19 pneumonia from portable chest X-ray images. Neurocomputing, 481, 202-215.
21. Farhan, A. M. Q., & Yang, S. (2023). Automatic lung disease classification from the chest X-ray images using hybrid deep learning algorithm. Multimedia Tools and Applications, 1-27.
22. https://www.kaggle.com/datasets/tawsifurrahman/covid19-radiography-database